Complex three-dimensional rearing environments amplify compensatory plasticity following early blindness

Abbreviated title: Enrichment shapes plasticity after early blindness

Deepa L. Ramamurthy[1, 2, *], Mackenzie Englund[1], Tanner J. Kovacs[1,3], Heather Dodson[1], Leah A. Krubitzer[1].

[1]Center for Neuroscience, University of California, Davis, Davis CA 95618

[2]Current Affiliation: Department of Psychology, 900 University Ave, Riverside, CA 92521

[3]Current Affiliation: University of Nebraska Medical Center, 42nd and Emile Streets Omaha, NE 68198

***Corresponding Author**: Deepa L. Ramamurthy, deepar@ucr.edu

Author contributions: D.L.R. and L.A.K. designed the study. D.L.R., M.E., T.J.K., and H.D. performed the experiments. D.L.R. analyzed the data. D.L.R. and L.A.K. wrote the manuscript.

Number of Figures: 5, **Tables**: 3, **Extended Data Figures**: 3, **Extended Data Tables**: 3

Number of Words for Abstract: 249, **Introduction**: 750, and **Discussion**: 1059

Funding Sources: This research was supported by NIH NEI 5R01EY034303 and James S. McDonnell Foundation grant 220020516 to L.A.K and NSF GRFP DGE-1650042 to D.L.R.

Conflicts of interest: None

Acknowledgments: We thank Dr. Cindy Clayton for animal care, Carly Jones for assistance with preliminary data analysis, and Carlos Pineda for comments on a draft of this manuscript.

ABSTRACT

The neocortex has a remarkable capacity to alter its functional organization and connectivity in response to sensory loss, particularly if this loss occurs early in life. A key question is whether this cross-modal reorganization is driven by sensory deprivation or by enhanced use of the spared senses. We investigated how different rearing environments shape neural responses in primary somatosensory cortex (S1) of short-tailed opossums (*Monodelphis domestica)*, following elimination of visual inputs through bilateral enucleation in early development. Early blind and sighted littermates were reared in enriched environments to promote active tactile exploration in three-dimensional (3D) space, or in standard laboratory cages. In adulthood, both enriched groups showed adaptive changes in exploration patterns and gap crossing behaviors relative to standard-reared counterparts. Thus, early blind animals showed behavioral compensation when challenged by complex environments. Enriched rearing increased selectivity of S1 neural responses to whisker touch and altered receptive field shapes such that they were less horizontally anisotropic. This shift was strongest in enriched early blind animals, enhancing tuning along the behaviorally relevant horizontal axis more than in standard-reared early blind animals. Thus, alterations in receptive fields of neurons in S1 following early blindness were amplified by environmental complexity. Sighted opossums reared with enrichment also showed similar whisker receptive field plasticity, though to a slightly lower degree. Together, these results demonstrate the strong influence of the rearing environment on reorganization of cortex that processes inputs from the spared senses, underscoring the role of experience in directing compensatory plasticity following early sensory loss.

SIGNIFICANCE STATEMENT

Enhanced perceptual abilities following early sensory loss are often attributed to cross-modal recruitment of cortex linked to the deprived sense. However, plasticity also occurs within cortical areas representing spared modalities. It remains unresolved whether deprivation alone is sufficient to induce such reorganization, or whether experience using the spared sense is required. We show that enriched rearing amplifies neural coding changes in primary somatosensory cortex after early blindness, shaping receptive field geometry and promoting adaptive behavioral strategies aligned with environmental demands. Comparable changes in sighted animals reared under the same conditions reveal that reliance on touch—rather than visual deprivation alone—drives this neural and behavioral plasticity, supporting the critical role of experience in enhancing functional outcomes after early sensory impairment.

INTRODUCTION

Early loss of vision leads to heightened perceptual abilities in the remaining senses, accompanied by structural and functional brain plasticity (Goldreich and Kanics, 2003; Wong et al., 2011; Voss, 2011; Morland et al., 2021; Mezzera and López-Bendito, 2016; Lazzouni and Lepore, 2014). However, the developmental origins of this plasticity remain poorly understood, particularly the extent to which sensory experience, movement options and affordances contribute to compensatory changes in brain and behavior. In this study, we investigate how enhancing tactile experience through rearing in an enriched environment contributes to neural and behavioral plasticity of whisker-mediated touch in a marsupial, the short-tailed opossum, when vision is lost early in development.

Exposure to enriched environments drives plasticity in sensory cortices of juvenile and adult animals with intact brains and bodies. This includes functional reorganization of sensory representations through changes in cortical territory, neuronal response properties (latency, strength, and selectivity), neuronal morphology and molecular expression (Seo, 1992; Leah et al., 1985; Coq and Xerri, 1998; Cancedda et al., 2004; Engineer et al., 2004; Polley et al., 2004; Guic et al., 2008; Mégevand et al., 2009; Devonshire et al., 2010; Alwis and Rajan, 2013, LeMessurier et al., 2018, Bibollet-Bahena 2023). Enrichment also counteracts degradation of representations after transient sensory deprivation, and promotes recovery from brain injury (Polley et al., 1999; Bartoletti et al., 2004; Sale et al, 2007; Nakashima and Dyck, 2008; Wang et al., 2013; Greifzu et al., 2014; Zhu et al., 2014; Zheng et al., 2014; Jiang et al., 2015; Kalogeraki et al., 2017; Levine et al., 2017). Rearing animals in naturalistic environments aligned with a species' lifestyle engages ethologically relevant behavior (Landers et al., 2011; Wilkinson et al, 2010; Branchi et al., 2011; Weissbrod et al, 2013) and is especially effective in reshaping cortical sensory representations at structural, functional and molecular levels (Polley et al., 1999; Polley et al., 2004; Frostig, 2006; Gomez-Pinilla et al., 2011; Landers et al., 2011). Here, we therefore used a complex three-dimensional rearing environment designed to model aspects of the natural habitat and lifestyle of short-tailed opossums.

Many small mammals, including short-tailed opossums, routinely use forest habitats across vertical strata, from floor to canopy (Jenkins, 1974; Jones et al., 2003; Delciellos and Vieira, 2006; Abreu and Oliveira, 2014; Shapiro et al., 2014). Short-tailed opossums are terrestrial hunters and foragers (Jones et al., 2003) but prefer nesting

above ground in rocky outcrops (Macrini, 2004), using branches and logs as arboreal runways to negotiate complex terrain (Lammers, 2007; Lammers and Gauntner 2008; Ladine and Kissel, 1994; Montgomery, 1980). They are skilled climbers despite lacking morphological specializations of arboreal species, relying on behavioral strategies to maintain balance and traverse arboreal substrates (Saunders et al., 1995; Saunders et al., 1998; Wilkinson et al., 2010; Schmitt et al., 2010; Rupert et al., 2014; Goin et al., 2016; Thomas et al., 2017; Lammers, 2004; Lammers, 2007; Lammers, 2009; Lammers and Biknevicius, 2004; Lammers et al., 2006; Lammers and Gauntner, 2008). Whisker touch is critical for navigating spatially complex 3D environments (Ahl, 1986; Arkley et al., 2017), guiding gap crossing and forelimb placement (Arkley et al., 2014; Niederschuh et al., 2015; Arkley et al., 2017; Grant et al., 2018). Peripheral organization of the whisker system reflects lifestyle demands and is more developed in arboreal than terrestrial species; in short-tailed opossums, whisker layout is consistent with semi-arboreal and scansorial marsupials (Beddard, 1902; Pocock, 1914; Lyne, 1958; Lyne, 1959; Muchlinski, 2013; Grant et al., 2017; Grant et al., 2018; Ramamurthy and Krubitzer, 2016; Grant et al., 2013). Thus, vertical environmental use depends heavily on behavioral modifications guided by tactile input (Lammers and Biknevicius, 2004; Lammers, 2009).

Early loss of visual inputs in short-tailed opossums at P4, prior to the formation of retinogeniculate and thalamocortical pathways, enhances tactile acuity and alters neural coding of whisker inputs in primary somatosensory cortex (S1), with receptive fields exhibiting greater selectivity along the principal axis of whisker motion (Ramamurthy & Krubitzer, 2018). Further, there is major reorganization of thalamic and cortical connections of somatosensory cortex relative to sighted animals (Dooley & Krubitzer,

2019). This raises a critical question: are alterations in somatosensory coding driven primarily by deprivation-induced anatomical reorganization, or by tactile experience itself? Here, we implement rearing conditions that encourage naturalistic tactile exploration in a spatially challenging environment designed to increase reliance on whisker use. By comparing how an enriched environment shapes neural coding and behavior related to whisker touch in sighted and early blind animals, we interrogate the role of tactile experience in directing compensatory plasticity following early blindness.

MATERIALS AND METHODS

Animals

Thirty-three adult short-tailed opossums of either sex (*Monodelphis domestica*; age range: 4-16 months; weight range: 61-165g) were used for electrophysiological recording experiments. Animals belonged to four experimental groups (**Table 1**), early blind and sighted reared in two conditions (standard: ‘s’, enriched: ‘e’). Previously published data from standard-reared animals were reanalyzed for comparison with enriched rearing groups (Ramamurthy and Krubitzer, 2018).

Ethics Statement

All protocols were approved by the Institutional Animal Care and Use Committee, and experiments were conducted according to the criteria outlined in the National Institutes of Health *Guide for the Care and Use of Laboratory Animals*.

Bilateral enucleation

For early blind opossums, bilateral enucleations were performed at P4 (**Figure 1**). Mothers of experimental litters were lightly anesthetized with Alfaxan (initial dose: 20

mg/kg; maintenance doses: 10-50%; IM) to facilitate enucleation of the pups, which are attached to the mother at this developmental stage. Pups were anesthetized by hypothermia. Health of both the mother (respiration rate and body temperature) and the pups (heartbeat, coloration and mobility) was monitored throughout the procedure. An incision was made in the skin covering the eyes, the eyes were removed under microscopic guidance, and the skin was repositioned and resealed using surgical glue. Approximately 50% of each litter was bilaterally enucleated and the remaining littermates served as sighted controls. After complete recovery from anesthesia, mothers along with their attached litters were placed into either standard or enriched housing, depending on the experimental group.

Rearing paradigms

Mothers of all experimental groups were reared and housed in standard laboratory cages until bilateral enucleations were performed on the pups at P4. Following the enucleation procedure, mothers with litters belonging to the standard rearing groups were placed in standard laboratory cages, while those belonging to the enriched rearing groups were placed in custom-made enriched cages (**Figure 1-1**). All animals were maintained on a 14/10 light/dark cycle. Food and water were available *ad libitum* in the cage under both rearing conditions. All experimental litters were housed together with the mother until weaning at ~8 weeks (P56), and at that stage they were separated from the mother, but the whole litter continued to be housed together until adulthood at ~4 months (P120). Adults (>P120) were individually housed under standard rearing conditions, but in groups of 2-4 same-sex littermates under enriched conditions (see below).

136 Standard rearing: Under standard rearing conditions, adult animals were singly housed
137 in standard laboratory cages, in cages similar to those typically used for laboratory
138 rodents (cage dimensions: 18.5”l x 10”w x 8”h). The home cage was provided with a
139 nesting cup and nesting material (shredded paper towels).

140 Enriched rearing: The enriched rearing environment in our study incorporated features
141 common to environmental enrichment (EE) paradigms previously used in rodents
142 (Nithianantharajah and Hannan, 2006; Sale et al., 2009; Bengoetxea et al., 2012), and
143 additionally takes into consideration the natural lifestyle of short-tailed opossums (**Figure**
144 **1-1**). Juvenile animals were cohoused until weaning with the mother as well as littermates,
145 and then with just their littermates from weaning until adulthood, as described above.
146 Enriched cages were provided with standard bedding and nesting material, as well as
147 some additional nesting material with a different texture. In addition to the nesting cup
148 placed on the floor as in standard cages, enriched cages provided the option of nesting
149 high above the cage floor, in nesting boxes attached to the cage walls. A single nesting
150 box was provided in the cage at juvenile stages of the experimental litters. In adulthood,
151 balanced numbers of eSC and eEB littermates were housed together in each enriched
152 cage, with a maximum of four opossums per cage. Each adult animal was provided with
153 an individual nesting box. Unlike common enrichment paradigms, which typically
154 incorporate toys into standard cages, the enriched cages used here were substantially
155 larger (~8x in volume; 29”l x 18”w x 24”h) compared to standard cages to encourage
156 tactile exploration in all three dimensions. The greatest increase relative to standard
157 cages was along the vertical dimension: enriched cages were 3x taller than standard
158 cages. Enrichment toys (Bio-Serv) of different shapes and textures were provided in the

159 cage. Toys were replaced, and the positions of manzanita branches were changed every
160 2–3 days to introduce novelty and promote continual exploration of the environment.

161 **Behavioral testing**

162 Arena testing: Arena testing was performed in three adult animals from each of the four
163 experimental groups. The arena consisted of a cage with the dimensions of enriched
164 cages, containing a single nest box near the top of the arena, with a branch leading up to
165 it. Animals were placed in the arena and allowed to explore it for 5 minutes in complete
166 darkness, and movies of their behavior were acquired under infrared (IR) illumination.
167 idTracker software (**Figure 2-1A**; Romero-Ferrero et al., 2019) was used to extract
168 movement trajectories of individual animals, which was further analyzed in MATLAB. In
169 each movie frame, we segmented the arena into a vertical zone (cage walls, branches,
170 and nest area) and a horizontal zone (cage floor). Exploratory activity was quantified from
171 session-wise binarized matrices (1280 × 720 pixels; height × width) containing the
172 animal's position in each frame. To assess differences in how animals sampled vertical
173 space in the arena, binarized occupancy maps were summed across sessions separately
174 for standard- and enriched-reared animals and collapsed along the horizontal axis,
175 yielding a per-row estimate of vertical occupancy. Vertical occupancy profiles were then
176 binned in 20-row increments (20 px per bin; vertical dimension only) and normalized to
177 the percentage of total vertical occupancy (summing to 1 across the vertical axis). For
178 each animal, total vertical occupancy (V) and horizontal occupancy (H) were computed
179 by summing binarized pixel values within the corresponding zone across all frames. A
180 normalized vertical preference index was calculated for each animal as:

$$Vertical\ Preference\ \ Index = \frac{(V - H)}{(V + H)}$$

Additional analysis of exploratory behavior in the arena test was performed through manual scoring in BORIS (Behavioral Observation Research Interactive) software. All home cage behavior data were analyzed offline by four independent observers such that multiple epochs were scored by at least two independent observers with a high interrater reliability (Cohen's κ coefficient of > 0.85; κ = 0 indicates no agreement in scoring between observers and κ = 1 indicates perfect agreement; Ramamurthy & Krubitzer, 2018; Landis and Koch, 1977). Arena exploration was initially scored using a binary scale of active states (locomotion bouts) and inactive states (resting bouts). A switch between an active and inactive state was only considered to have occurred if a bout lasted for at least 5 s. Active states were then further scored for crossing events that occurred during natural exploration of the arena. Crossing events were defined as instances in which an animal crossed from one surface to another within the arena. Four types of crossing events were scored: (1) floor to wall/wall to floor (2) wall to wall (3) floor to branch/branch to floor (4) nest or branch to wall/wall or branch to nest. Since systematic differences were not observed across crossing event types, only combined summary plots are shown.

Gap crossing task: Gap crossing was tested in 3-4 adult animals per experimental group. Animals were allowed to spontaneously cross from one platform (“start”) to another platform (“goal”) with either small (2-10 cm) or large gap distances (12-14 cm) separating them, which were interleaved in a pseudorandom order. Animals were tested for 7 days with intact whiskers, followed by 1-3 days of testing after whisker trimming. On each trial animals were allowed to remain on the start platform and attempt crossing for a maximum

203 of 1 minute. If no crossings were performed, the trial was ended, and animals were
204 removed from the platform for 1 min before returning to the platform for the next trial.
205 Movies of this behavior were acquired under IR illumination or dim red light, and
206 DeepLabCut was used for analysis of gap crossings (**Figure 2-1B-C**). The snout tip, the
207 base of the tail and the position of the edges of each platform were labeled in a subset of
208 frames to generate the dataset (260 frames across 13 opossums) on which the network
209 was trained (200,000 iterations). On a subset of trials, slow-motion movie clips in a
210 zoomed-in field of view were acquired to visually confirm the use of whiskers during gap
211 crossing. Infrared motion sensors (emitter/detector pairs) placed on either side of the
212 edge of each platform detected beam breaks and beam break times were recorded as a
213 secondary method of confirmation.

214 **Surgical procedures**

215 Animals were anesthetized with urethane (initial dose: 1.25 g/kg, 30% in saline, IP;
216 supplemental doses: 0.125-0.313 g/kg, 30% in saline, IP). Vital signs (respiration and
217 body temperature) were monitored throughout the experiment. At the beginning of the
218 surgery, dexamethasone (0.4-2.0 mg/kg; IM) was administered to minimize intracranial
219 swelling. Lidocaine (2% solution; SC) was injected at the midline of the scalp and around
220 the ears. The animal was then placed in a stereotaxic frame. Following an incision at the
221 midline of the scalp and retraction of the temporal muscle, a craniotomy was performed
222 to expose the entire parietal cortex and the dura was retracted. The surface of the
223 neocortex was covered with a layer of silicone fluid to prevent desiccation and then
224 photographed so that electrode penetration sites could be related to patterns of
225 vasculature. After the craniotomy, the animal was removed from the stereotaxic frame to

226 permit full access to the face for whisker stimulation. Three stainless steel skull screws
227 were inserted in the skull contralateral to the recording electrode. The head of the animal
228 was stabilized by cementing a head post to the skull screw in a rostral location over the
229 cortex. The other two skull screws were inserted epidurally into the skull over the
230 cerebellum and over the olfactory bulbs, serving as the reference and ground electrodes,
231 respectively, and also providing additional anchoring support for the dental cement.

232 **Extracellular recordings and whisker stimulation**

233 Somatosensory receptive fields were first coarsely mapped by recording multiunit
234 activity while applying tactile stimuli using a handheld probe. The representation of the
235 whiskers in S1 was localized by progressively testing electrode penetration sites medial
236 to the rhinarium representation and caudal to the lower jaw/lip representation. After this,
237 when receptive fields were found to be located on the mystacial or genal whisker pad
238 (Ramamurthy & Krubitzer, 2016), computer-controlled whisker deflections were used to
239 quantitatively measure single unit receptive fields.

240 Whisker stimuli consisted of single whisker deflections (2°) delivered using
241 piezoelectric actuators (4 ms/100 ms/4 ms ramp-hold-return; 5 mm from the whisker
242 base; 1.4 mm forward excursion). Data were collected for a grid of sixteen whiskers on
243 the mystacial pad to enable construction of somatotopic receptive fields. Whiskers were
244 deflected in a pseudorandom order with 50-100 trials collected per whisker (in blocks of
245 3-50 trials) at each recording site. Extracellular recordings (amplifier gain: 10,000X; A-M
246 Systems Model 1800 Microelectrode AC Amplifier; A-M Systems, Carlsborg, WA;
247 sampled at 28 kHz; Power1401, Cambridge Electronic Design Limited, Cambridge, UK)
248 were made 400-500 μm below the pial surface using monopolar tungsten microelectrodes

249 (FHC, Inc., Bowdoin, ME; 1-5 MΩ at 1 kHz) lowered with a hydraulic microdrive (David
250 Kopf Instruments, Tujunga, CA). Recordings were bandpass filtered (300-3000 Hz), and
251 spike-sorting was carried out offline to confirm isolation of single units. After
252 electrophysiological data was collected, fluorescent probes were used to mark the
253 location of recording sites, so that these could be related to histologically identified cortical
254 field boundaries (**Figure 3-1**).

255 **Histology**

256 At the end of each experiment, animals were injected with an overdose of sodium
257 pentobarbital (Beuthanasia; 250 mg/kg IP) and transcardially perfused with 0.9% saline,
258 followed by 2-4% paraformaldehyde in phosphate buffer, and then 2-4%
259 paraformaldehyde in 10% phosphate-buffered sucrose. The brain was extracted and
260 post-fixed (1-2 hours in 4% paraformaldehyde in 10% phosphate-buffered sucrose). In
261 some cases, the cortical hemispheres were flattened and the tissue was sectioned
262 tangentially at 30 μm using a freezing microtome, and then processed for myelin staining
263 (Gallyas, 1979; Dooley et al, 2013) to enable reconstruction of cortical field boundaries.
264 Reconstructions were drawn using Adobe Illustrator CS5 (Adobe, San Jose, CA). Digital
265 images of processed tissue were obtained using either a Nikon Multiphot system or an
266 Optronics MicroFire digital microscope camera. Contrast and brightness of whole images
267 were adjusted using Adobe Photoshop CS5 (Adobe, San Jose, CA).

268 **Neural data analysis**

269 Data files were processed blind to experimental group identity. Single-unit isolation
270 was performed while running the experiment using template-matching procedures in
271 Spike2 (Cambridge Electronic Design Limited, Cambridge, UK; RRID:SCR_000903), and

unit isolation was verified offline in Spike2, using principal component analysis. Stable waveforms and firing rates over the course of the recording session, and <0.5% refractory period violations (interspike interval <1.5 ms) were required for units to be included in the analysis. Spike times were then exported to MATLAB (Mathworks, Inc., Natick, MA; RRID:SCR_001622) and analyzed using custom scripts. Whisker evoked firing rates were measured as the spike count following stimulus onset (0-100 ms) and were considered significant if they exceeded prestimulus spike counts in an equivalent time window by two standard deviations. The *best whisker* (BW) was defined as the whisker with the highest evoked response, and depending on their proximity to the BW the remaining whiskers were categorized as *first-order surround whiskers* (1° SW; immediately adjacent to BW), *second-order surround whiskers* (2° SW; one position removed from BW) and *third-order surround whiskers* (3° SW; two positions removed from BW).

One measure of receptive field size used was the number of whiskers that evoked a significant response in each recorded neuron. Another measure used was the rank-ordered whisker tuning curve for each neuron, where responses to all whiskers tested were sorted in descending order of whisker-evoked response magnitude, and normalized to peak (BW response). Further, mean 2D somatotopic receptive fields were obtained after normalizing SW-evoked response magnitudes to the BW-evoked response, and aligning receptive fields of single units such that the BW was at the center of the receptive field for each unit. Because *Monodelphis* lacks discrete anatomical cortical barrels (Ramamurthy & Krubitzer, 2016), 2D receptive fields were aligned relative to the BW position rather than an anatomically defined “principal whisker” or “columnar whisker”. 50, 75, and 90% contour lines (for response levels relative to the BW) were plotted for the

295 mean receptive fields (smoothed by linear interpolation) to facilitate visualization. Raw
296 values were used for all calculations and statistical comparisons.

297 We define anisotropy in receptive fields as the difference in the tuning width of an
298 S1 neuron's receptive field when measured along different spatial directions of the
299 whisker pad—across arcs (horizontal axis) and across rows (vertical axis). Anisotropies
300 in the structure of somatotopic receptive fields were quantified as the *shape index:*

301 $$Shape\ index = \frac{(Row\ tuning\ width\ index - Arc\ tuning\ width\ index)}{(Row\ tuning\ width\ index + Arc\ tuning\ width\ index)}$$

302 If the sum of the row and arc tuning width indices was zero, the shape index was
303 assigned to be zero. Shape indices ranged from -1 to 1, with values >0 indicating broader
304 tuning along the row compared to the arc (i.e. broader horizontal tuning), and values <0
305 indicating broader tuning along the arc compared to the row (i.e. broader vertical tuning).
306 Neuronal selectivity for the best whisker along the row and arc dimensions was measured
307 by assessing tuning width separately along the horizontal and vertical axes as the *row*
308 *tuning width index* and the *arc tuning width index* respectively, either considering only 1°
309 SW, or 1°, 2°, 3° SW in the row or arc of the BW, as stated below:

310 $$Row\ tuning\ width\ index = \frac{(\text{Mean evoked response of } SW_{row})}{\text{BW evoked response}}$$

311 $$Arc\ tuning\ width\ index = \frac{(\text{Mean evoked response of } SW_{arc})}{\text{BW evoked response}}$$

Additionally, the *whisker selectivity index (WSI)* for BW vs. in-row or in-arc whiskers was computed separately for each neuron, considering BW responses relative to 1°, 2°, 3° SW responses.

$$WSI_{row} = \frac{(BW\ evoked\ response - SW_{row}\ evoked\ response)}{(BW\ evoked\ response + SW_{row}\ evoked\ response)}$$

$$WSI_{arc} = \frac{(BW\ evoked\ response - SW_{arc}\ evoked\ response)}{(BW\ evoked\ response + SW_{arc}\ evoked\ response)}$$

In-row and in-arc selectivity indices ranged from 0 to 1, with values closer to 1 indicating higher selectivity for the BW in the corresponding dimension.

Receptive field shape was quantified at two spatial scales (1° only vs. 1°-3°) because somatotopic receptive fields of neurons in the S1 whisker representation consist of the BW (peak response) and a graded, multi-whisker surround shaped by intracortical integration, including anisotropies along row vs. arc axes. This receptive field organization has been demonstrated in classical mouse and rat studies (e.g., Simons, 1978; Brecht & Sakmann, 2002; Fox, 2008), as well as prior work demonstrating similar receptive field structure in opossum S1 (Ramamurthy & Krubitzer, 2016; Ramamurthy & Krubitzer, 2018).

Since receptive field shape analysis characterizes the overall geometry of the field around the BW, it cannot be meaningfully computed for a non-continuous portion of the surround alone (e.g., only 2°/3° SWs); therefore 2°/3° were not analyzed separately from 1° SWs; instead, shape analyses with only 1° SWs characterized local receptive field

configuration, whereas analyses including 1°-3° SWs captured receptive field configuration shaped by broader spatial integration.

Statistical Analysis

Statistical analyses were performed in MATLAB and R. Permutation tests for the difference in medians were used to assess differences between two groups (referred to in brief as 'permutation test'). Fisher's exact tests (two-sided) were used for analyses of 2x2 contingency tables to compare proportions across conditions. All statistical tests for neuronal data use 'n' of cells. We accounted for interindividual variability using linear mixed effects models.

To model crossing behavior in the gap-crossing task, we fit a generalized linear mixed-effects model using 'fitglme' in MATLAB (Poisson distribution; log link). Crossing counts were modeled with the log of observation time included as an offset to estimate rates. Fixed effects included experimental group, gap size, whisker trimming, and the interactions of experimental group with gap size and with whisker trimming, respectively. Since whisker trimming abolished crossings on 100% of large-gap trials, those trials were excluded from this analysis. Animal identity was included as a random intercept (1|ID) to account for repeated measures. The model specification was as follows:

$$Response\ Variable \sim Experimental\ Group * Gap + Experimental\ Group * Trim + (1|Animal\ ID)$$

The model was estimated using the Laplace approximation for maximum likelihood. Overdispersion was evaluated via Pearson dispersion; if dispersion exceeded 1.5, we added an observation-level random effect (1|Obs) to handle overdispersion.

To analyze gap crossing durations on successful trials we fit a linear mixed-effects model using 'fitlme' in MATLAB with the specification:

$$Response\ Variable \sim Experimental\ Group * Gap + Experimental\ Group * Trim + (1|Animal\ ID)$$

where experimental group and test condition were modeled as fixed effects, and animal ID modeled as a random effect.

Planned post hoc comparisons for both models were performed using coefTest with contrast matrices for group and condition effects (gap size and whisker trimming), including a difference-in-differences contrast for the blindness × environment interaction. 'coefTest' returned p-values for each contrast, with Satterthwaite degrees of freedom applied where applicable.

For neural data, experimental group was modeled as a fixed effect and animal identity as a random effect, using the model specification:

$$Response\ Variable \sim Experimental\ Group + (1|Animal\ ID)$$

Planned contrasts were performed using 'coefTest' for pairwise group comparisons and for a difference-in-differences (blindness × environment) contrast, with p-values returned and Satterthwaite degrees of freedom applied where applicable. Additional models were fit for key analyses with sex included as a fixed effect to test for differences between males and females, but no significant sex differences were identified.

Exact p-values for fixed effects of experimental group and/or test condition (gap size/whisker trimming) obtained from Poisson and Gaussian generalized linear mixed-

372 effects models, or from Fisher's exact tests for categorical comparisons, with pairwise
373 contrasts across experimental groups are provided in **Table 2** and **Table 3.**

374 **RESULTS**

375 **Behavioral adaptations of blind and sighted opossums in enriched rearing**
376 **environments**

377 In short-tailed opossums, postnatal day 0 (P0) is developmentally equivalent to
378 embryonic stages in rodents (approximately E11 in mouse and E12 in rat; Molnár and
379 Blakemore, 1995; Molnár et al., 1998). Bilateral enucleations were conducted at P4,
380 before retinal afferents and thalamocortical axons reached their respective targets (Taylor
381 and Guillery, 1994; Molnár et al., 1998), completely eliminating both spontaneous retinal
382 activity and visually evoked input (**Figure 1)**. Following bilateral enucleation on postnatal
383 day 4, opossum mothers and their litters, including sighted and blind pups, were
384 transferred into a new standard or enriched home cage environment (**Figure 1**; **Figure 1-**
385 **1A-D**). Prior to P12, sensory experience in either environment was determined entirely
386 by behavioral patterns of the mother, due to the obligate attachment of opossum pups.
387 Juvenile animals continue to rely on the mother for both sustenance and transportation
388 until weaning at P56, but with increasing independent exploration (**Figure 1-1E-F**).
389 Opossum mothers always preferentially nested high above the ground (n = 3 mothers,
390 producing a total of 4 enriched experimental litters; example in **Movie 1**), so pups were
391 forced to rely heavily on touch to navigate the enriched environment. By adulthood, both
392 sighted and early blind animals were highly adapted to their environments (**Movie 2-3**).

393 To assess how rearing condition and visual condition (blind versus sighted) shape
394 exploratory behavior, we tested each group in a novel arena matching the dimensions

395 and basic layout of the enriched home cages (**Figure 2; Figure 2-1A**). We quantified
396 spatial sampling preferences (**Figure 2A-C** and **2E**), overall locomotor activity (**Figure 2D**
397 and **2F**), and spontaneous crossings between surfaces during natural exploration (**Figure**
398 **2D** and **2G**), capturing both spatial and temporal aspects of behavior. These measures
399 contextualize and complement the more controlled gap crossing behavior assay
400 presented in the next section. Movement trajectories were highly similar for sighted and
401 blind animals within each rearing condition (**Figure 2A-B**; **Figure 2-1A**), consistent with
402 successful behavioral compensation by blind animals even in more spatially complex
403 environments. In contrast, rearing environment strongly impacted how animals sampled
404 the novel arena: enriched opossums explored vertical space more extensively than those
405 reared in standard cages ($p = 0.018$, permutation test; **Figure 2C**; **Figure 2E**), though
406 overall activity levels ($p=0.565$, permutation test) and durations of naturally occurring
407 crossing events were not significantly different ($p=0.232$, permutation test; **Figure 2D**;
408 **Figure 2F-G**). Quantifying gap crossing during free exploration has some limitations
409 which may mask differences in sensory-mediated behavior. Crossing events that
410 occurred during free exploration, where animals crossed from surface to surface did not
411 necessarily involve crossing of discrete gaps, and we could not control for gap size across
412 different crossing events. Further animals were free to adopt varying postures prior to
413 crossing, and to use varying behavioral strategies involving sensory inputs from multiple
414 body parts to aid gap crossing during free exploration.

415 To assess sensorimotor performance under more precisely defined task
416 parameters, we used a gap crossing task (conducted in darkness) in which gap size was
417 systematically varied across trials, animals had only one possible path forward (across

418 the gap), and the constraints of the apparatus required animals to adopt a standardized
419 posture prior to gap crossing (**Figure 3A**; **Figure 2-1B-C**). Crossing large gaps required
420 whisker use, as the goal platform was out of reach from the start platform except through
421 whisker contact. We quantified (1) the fraction of trials resulting in a successful crossing
422 (**Figure 3B**), (2) crossing rates over time (**Figure 3C**), and (3) the duration of successful
423 crossing events (**Figure 3D**).

424 The fraction of successful trials (i.e. the probability of success) was strongly
425 impacted by gap size (sSC: 8%, sEB: 14%, eSC: 17%, eEB: 14%; percent successful
426 trials, in comparison to 100% success on small gap trials) and by whisker trimming
427 (**Figure 3B**, Fisher's exact test, $p < 0.001$; see **Table 2** for exact p-values for the fixed-
428 effect of experimental group, and for all pairwise comparisons between groups),
429 eliminating successful crossings at large gaps for all experimental groups. This is
430 consistent with the role of whiskers in gap crossing described in previous studies of small
431 mammals (Hutson & Masterton 1986, Voigts et al., 2015, Arkley et al. 2017, Graham &
432 Socha 2020, Toso & Diamond 2023). All animals crossed on 100% of small gap trials,
433 with or without whiskers, indicating that other body parts also contributed to small gap
434 crossings.

435 Crossing rates, which reflect success rate normalized by time, were significantly
436 lower for large gaps than for small gaps within each experimental group (**Figure 3C,**
437 **Table 2**, **Table 3-1**; $p < 0.001$ in all cases, all p-values from Poisson generalized linear
438 mixed-effects model) with no significant differences across groups ($p>0.05$). Although
439 there was a trend toward decreased crossing rates in all experimental groups with whisker
440 trimming, trimming effects were not statistically significant for crossing rates ($p>0.05$).

The third metric in the gap crossing task was the duration of successful crossings (**Figure 3D**, **Table 2**, **Table 3-1**). We observed significant fixed effects of experimental group ($p < 0.001$; all p-values from the linear mixed effects model), gap size ($p < 0.001$), and whisker trimming ($p < 0.001$), as well as interactions between group and gap size ($p < 0.001$) and between group and trimming ($p = 0.01$). Across groups, successful crossings were generally slower for large versus small gaps, with modest but significant increases in crossing times on small gaps after whisker trimming (with one exception; see below). Consistent with **Figure 3B**, this pattern suggests primary reliance on whiskers for large gaps, whereas small gaps can be crossed using strategies that incorporate both whiskers and tactile inputs from other body parts (Ramamurthy et al., 2021).

Group differences based on visual condition and rearing condition were most pronounced for large gaps (**Figure 3D**). Early blind opossums crossed large gaps faster than sighted controls under standard rearing (sSC vs. sEB: $p < 0.001$), and this advantage was amplified by enriched rearing (eEB vs. sEB: $p < 0.001$). Both enriched groups were significantly faster than standard-reared animals ($p < 0.001$ for all pairwise comparisons), with enriched blind animals outperforming enriched sighted animals ($p < 0.01$). Enriched blind animals followed the general trends of other groups but were the only cohort without a significant difference between large and small gap durations ($p > 0.05$), reflecting comparatively faster large gap performance. They were also the only group in which whisker trimming did not significantly prolong small gap crossings ($p > 0.05$). Taken together, these results indicate heightened performance supported by whisker use on large gaps, along with adaptive recruitment of other body parts to maintain small gap performance when whiskers are absent.

464 **Tactile experience amplifies compensatory neural plasticity in blind opossums**

465 Single-unit recording experiments were performed in 19 opossums reared in
466 standard conditions (10 sSC, 9 sEB), and 14 opossums reared in enriched conditions (7
467 eSC, 7 eEB), acquiring data for a total of 339 neurons across experimental groups (see
468 **Table 1**; **Figure 3-1**). 63-73% of units recorded in S1 (sSC: 60, sEB: 64, eSC: 58, eEB:
469 51) had a significant evoked response (>2 SD above baseline) to stimulus onset following
470 single whisker deflections, and these neurons were included in receptive field analyses.
471 Raster plots and peristimulus time histograms (PSTHs) for whisker-responsive neurons
472 in each group are shown in **Figure 4A-B**. These examples illustrate more selective
473 whisker touch responses in standard-reared blind opossums, with selectivity further
474 amplified in enriched groups.

475 In general, spontaneous firing rates of S1 neurons were low, consistent with
476 previously reported findings in standard-reared animals (Ramamurthy and Krubitzer,
477 2018), and were not significantly different among experimental groups (**Figure 4C**, **Table**
478 **3**, **Table 4-1**; mean ± SEM, sSC: 0.582 ± 0.083 spk/s, sEB: 0.613 ± 0.121 spk/s, eSC:
479 0.544 ± 0.079 spk/s, eEB: 0.503 ± 0.082 spk/s; linear mixed-effects model, $p>0.05$; see
480 **Table 3** for exact p-values for the fixed-effect of experimental group, and for all pairwise
481 comparisons between groups). However, responses evoked by the stimulation of even
482 the most preferred single whisker stimulus (best whisker; BW) in enriched groups were
483 suppressed in relation to stimulus-evoked firing rates in standard-reared sighted
484 opossums (**Figure 4D**, **Table 3**, **Table 4-1**; mean ± SEM, sSC: 11.4 ± 0.839 spk/s, sEB:
485 8.39 ± 0.591 spk/s, eSC: 7.82 ± 0.748 spk/s, eEB: 4.57 ± 0.52 spk/s; linear mixed-effects
486 model, eSC vs. sSC: $p<0.01$, eEB vs. sSC: $p<0.001$), as previously reported in early blind

487 animals under standard rearing conditions (Ramamurthy and Krubitzer, 2018). Since
488 relative suppression of BW-evoked responses was observed in enriched sighted controls,
489 in addition to enriched early blind animals, this effect was not contingent on the lack of
490 vision itself – rather it was driven by increased dependence on touch in the enriched
491 groups of opossums. Mean BW-evoked firing rates in enriched sighted control animals
492 were comparable to those in standard early blind animals (linear mixed-effects model,
493 sEB vs. eSC: $p>0.05$). However, in enriched early blind animals, mean BW-evoked firing
494 rates were lower relative to all other experimental groups (linear mixed-effects model,
495 eEB vs. sEB: $p<0.001$, eEB vs. eSC: $p<0.001$, eEB vs. sSC: $p<0.001$). Thus, blindness
496 was not required for suppression of whisker-evoked responses, but the combination of
497 tactile enrichment and vision loss produced the greatest effect on whisker-evoked firing
498 rates of S1 neurons. This is consistent with animals relying on their whiskers to a greater
499 extent when reared in a complex environment in the absence of vision.

500 Average whisker receptive fields in both sighted and blind enriched groups were
501 significantly smaller than those in standard-reared sighted controls (mean ± SEM, eEB:
502 3.22 ± 0.409, eSC: 3.48 ± 0.364, sSC: 5.92 ± 0.427; linear mixed-effects model, eSC vs.
503 sSC: $p<0.001$, eEB vs. sSC: $p<0.001$) when measured as the number of whiskers that
504 evoked a significant response above spontaneous firing (**Figure 4E**, left, **Table 3**, **Table**
505 **4-1**). We see similar results when receptive fields are quantified as the mean rank-ordered
506 tuning curve across neurons (**Figure 4E**, right, **Table 3**, **Table 4-1**; linear mixed-effects
507 model, eSC vs. sSC: $p<0.001$). The finding that tactile enrichment in sighted control
508 animals leads to a decrease in mean receptive field size—similar to both standard-reared
509 and enriched early blind animals—supports the interpretation that this reduction reflects

510 an experience-dependent effect across all three groups. However, changes in measures
511 of overall receptive field size in enriched early blind animals relative to standard-reared
512 early blind animals were either not significant (**Figure 4E**, left, number of whiskers: eEB:
513 3.22 ± 0.409, sEB: 3.38 ± 0.270; linear mixed-effects model, eEB vs. sEB: $p>0.05$) or
514 modest (**Figure 4E**, right, rank-ordered tuning curve: linear mixed-effects model, $p<0.01$).
515 This suggests that, under standard rearing conditions, receptive field plasticity in early
516 blind animals may already have reached a limit that cannot be further shifted by
517 enrichment.

518 **Enrichment enhances selectivity for whisker touch along the behaviorally relevant**
519 **horizontal axis**

520 To better understand the effects of enriched rearing on receptive field configuration
521 of S1 neurons, we characterized two-dimensional receptive fields for the row (horizontal)
522 and arc (vertical) dimensions of the whisker pad (**Figure 5A**). Visual inspection of mean
523 2D receptive fields revealed clear differences in receptive field anisotropies across
524 experimental groups (**Figure 5B**). We quantified anisotropies in receptive fields as the
525 *shape index*, ranging in value from -1 to 1, where positive values indicated horizontally
526 anisotropic shapes, negative values indicated vertically anisotropic shapes and values
527 close to 0 indicated more isotropic shapes. Receptive fields for neurons in the S1 whisker
528 representation in standard-reared sighted control and early blind animals were dominated
529 by horizontally anisotropic shapes (**Figure 5C-D**, **Table 3**, **Table 5-1**). However, for early
530 blind animals reared in enriched conditions, the receptive field shape distributions were
531 shifted away from horizontal anisotropy – either when considering only 1° surround
532 whisker (SW) positions (**Figure 5C**; neurons with shape index > 0.0, sSC: 68.3%, sEB:

533 57.8%, eEB: 37.3%, Fisher's exact test, eEB vs. sSC: p=0.001, eEB vs. sEB: p<0.05;
534 linear mixed-effects model, eEB vs. sSC: p<0.001, eEB vs. sEB: p<0.05) , or when
535 including all SW (1° - 3°) positions (**Figure 5D**; neurons with shape index > 0.0, eEB:
536 37.3%, sSC: 81.7%, sEB: 76.6%, Fisher's exact test, eEB vs. sSC: p<0.001, eEB vs. sEB:
537 p<0.001; linear mixed-effects model, eEB vs. sSC: p<0.001, eEB vs. sEB: p<0.001).

538 Receptive field distributions were also shifted away from horizontal anisotropy in
539 sighted control animals reared in the enriched environment. This shift was not seen when
540 only 1° SW positions were considered (**Figure 5C**; neurons with shape index > 0.0, eSC:
541 55.2%, Fisher's exact test, eSC vs. sSC: p>0.05, eSC vs. sEB: p>0.05; linear mixed-
542 effects model, eSC vs. sSC: p>0.05, eSC vs. sEB: p>0.05) but becomes apparent when
543 1° - 3° SW positions are considered (**Figure 5D**; neurons with shape index > 0.0, eSC:
544 46.6%, Fisher's exact test, eSC vs. sSC: p<0.001, eSC vs. sEB: p<0.001; linear mixed-
545 effects model, eSC vs. sSC: p=0.01, eSC vs. sEB: p>0.05). Thus, rearing in an enriched
546 environment, which was permissive of more naturalistic patterns of tactile behavior,
547 shifted the shapes of receptive fields of S1 neurons away from the horizontally anisotropic
548 shapes typically found in animals reared in standard laboratory cages. The shift occurred
549 in both sighted and early blind enriched animals, but the effect was more pronounced in
550 early blind animals.

551 The results of receptive field shape analyses pointed to differential effects of
552 rearing environment on tuning along horizontal and vertical axes of receptive fields. We
553 quantified neuronal tuning width separately along whisker rows and arcs for each
554 experimental group (**Figure 5E**, **Table 3**, **Table 5-1**). Both sighted and early blind
555 enriched animals showed sharper tuning along both the vertical and horizontal axes

556 relative to sighted controls, but there was a striking difference in the magnitude of tuning
557 width changes along the horizontal vs. vertical axes.

558 This constitutes an amplification of shifts in receptive field anisotropies previously
559 described in early blind animals under standard rearing conditions (Ramamurthy and
560 Krubitzer, 2018). Along the arc (vertical) axis, tuning was sharpened to the same extent
561 in the enriched groups as seen in standard-reared early blind animals relative to sighted
562 controls (**Figure 5E**; %BW response for in-arc whiskers: eEB: 19.4 ± 2.80%, eSC: 18.7 ±
563 2.13%, sEB: 20.1 ± 1.58%, sSC: 26.7 ± 2.50%; linear mixed-effects model, eEB vs. sSC:
564 $p<0.05$, eEB vs. sEB: $p>0.05$, eSC vs. sSC: $p<0.05$, eSC vs. sEB: $p>0.05$). But along the
565 row (horizontal axis), both sighted and early blind enriched animals showed sharper
566 tuning relative to both groups of standard-reared animals (**Figure 5E**; %BW response for
567 in-row whiskers: eEB: 13.8 ± 2.07%, eSC: 20.9 ± 1.96%, sEB: 35.1 ± 2.82%, sSC: 49.1
568 ± 2.85%; linear mixed-effects model, eEB vs. sSC: $p<0.001$, eEB vs. sEB: $p<0.001$, eSC
569 vs. sSC: $p<0.001$, eSC vs. sEB: $p<0.001$). There was a trend for sharper row tuning in
570 enriched early blind animals compared to enriched sighted control animals, but this was
571 not significant (linear mixed-effects model; eSC vs. eEB: $p>0.05$). We computed the
572 whisker selectivity index as the normalized difference ratio of the neuronal response to
573 the best whisker in comparison to responses to in-row or in-arc whiskers. Population
574 distributions of the selectivity index for S1 neurons (**Figure 5F**, **Table 3**, **Table 5-1**) further
575 validate the anisotropy in the enhancement of selectivity seen for animals reared in
576 enriched environments (BW vs. in-arc whiskers: linear mixed-effects model, eEB vs. sSC:
577 $p<0.05$, eEB vs. sEB: $p>0.05$, eSC vs. sSC: $p<0.05$, eSC vs. sEB: $p>0.05$, eEB vs. eSC:

578 $p>0.05$; BW vs. in-row whiskers: linear mixed-effects model, eEB vs. sSC: $p<0.001$, eEB
579 vs. sEB: $p<0.001$, eSC vs. sSC: $p<0.001$, eSC vs. sEB: $p<0.001$, eEB vs. eSC: $p>0.05$).

580 Thus, a spatially complex enriched environment drives significantly greater
581 improvement in neuronal selectivity for whisker touch in early blind animals especially
582 along the rostrocaudal axis, which is the primary axis of natural whisking behavior. A
583 similar improvement in selectivity was observed in sighted control littermates reared in
584 the enriched environment, supporting the role of tactile experience rather than vision loss
585 itself in driving these effects. In summary, the results of our current study indicate that
586 compensatory effects on neural coding in S1 following early blindness do not arise solely
587 from visual deprivation and can be amplified and directed by tactile experience.

588 **DISCUSSION**

589 Although the effects of enrichment on plasticity within a sensory modality have
590 been studied at structural, functional, and molecular levels, few studies have examined
591 its impact on cross-modal compensatory plasticity, focusing mainly on c-fos expression
592 or synaptic changes (Piche et al., 2004; Mundiñano and Martínez-Millán, 2010; Zheng et
593 al., 2014). The short-tailed opossum is born with a highly immature nervous system,
594 enabling precise extrauterine manipulations at very early stages in development
595 (Ramamurthy and Krubitzer, 2018; Ramamurthy et al., 2021). Here, we tested the effects
596 of rearing sighted and early blind short-tailed opossums in a large and dynamic, spatially
597 complex 3D environment, and examined effects on tactile behavior and receptive field
598 configurations of neurons in S1.

599 Enrichment reduces abnormal stereotypic behaviors (e.g. overgrooming) and
600 other behavioral indicators of stress and aggression, and enhances learning, memory,
601 motor performance and social behavior (Dijkhuizen et al., 2024; Ratuski et al., 2024; Cait
602 et al., 2024; Nakhwa et al., 2024; Caires & Bossolani-Martins, 2023; Mieske et al., 2022;
603 Kentner et al., 2021; Khoo et al., 2020; Bailoo et al., 2018; Girbovan & Plamondon, 2013;
604 Amaral et al., 2008; Mason et al., 2007). It can also improve sensory function and
605 performance, including whisker touch discrimination (Zheng et al., 2021). In our study, we
606 implemented enrichment intended to increase the use of whisker touch. Since whiskers
607 are critical for guiding forelimb placement in crossing gaps when small mammals climb
608 (Ahl, 1986; Arkley et al., 2014; Niederschuh et al., 2015; Arkley et al., 2017; Grant et al.,
609 2018), we reared opossums in cages with periodically varying, spatially complex climbing
610 substrates and intermittently introduced novel toys, since novel objects and other
611 interactive enrichment devices promote active whisking behavior (Nakhwa et al., 2024;
612 Sofroniew & Svoboda, 2015). We show that in a novel setting, both sighted and blind
613 opossums showed differential exploration patterns reflecting the geometry of their rearing
614 environments. Additionally, enriched opossums are faster and more successful in gap
615 crossing using a whisker-dependent strategy. Thus, opossums use behavioral strategies
616 shaped by their rearing environments, and our enrichment approach effectively engages
617 and enhances naturalistic whisker-mediated behavior in both sighted and blind animals,
618 enabling us to evaluate the effects of enriched rearing on compensatory plasticity
619 following early vision loss.

620 It has been previously reported that early blindness alters the coding of whisker
621 touch inputs in opossums, in a manner that supports enhanced tactile discrimination

(Ramamurthy and Krubitzer, 2018; Ramamurthy et al., 2021). This involved suppression of whisker-evoked responses combined with increased spatial selectivity, due to the greater relative suppression of neural responses to non-preferred stimuli (SW) vs. the preferred stimulus (BW). These alterations in the receptive fields of neurons in S1 resemble the effects of naturalistic environmental enrichment on receptive fields of neurons in S1 of adult rats (Polley et al., 1999, 2004). Here we demonstrate that rearing early blind short-tailed opossums in an enriched environment further amplifies these changes. Since selectivity to whisker stimuli was enhanced not just in early blind animals but also in sighted control animals reared in enriched conditions, we can infer that suppression of whisker-evoked responses and increased selectivity of neural responses in the S1 whisker representation are effects of tactile experience rather than visual deprivation itself.

A key finding was the effect of the rearing environment on the shapes of receptive fields of S1 neurons – shape distributions for both sighted and early blind animals exhibited a prominent shift away from the horizontally anisotropic shapes that dominate in standard-reared opossums. This was accompanied by a reduction in tuning width along row (horizontal) vs. arc (vertical) axes in enriched animals – on average, tuning widths were reduced to a greater extent along the row axis, parallel to the main axis of whisker movements. This may reflect more naturalistic patterns of whisker use in short-tailed opossums, enabled by the increase in vertical space and availability of climbing substrates in the enriched rearing environment. In rats, simulations that modelled exploratory behavior predicted changes in the spatial patterns of whisker contact depending on the environment being explored (Hobbs et al., 2015) – whiskers within the

same horizontal row were more likely to come in simultaneous contact during exploration of flat surfaces, but in more complex and naturalistic environments, the probability distributions of simultaneous whisker contact shifted away from this row-wise structure. Such alterations in the patterns of tactile stimuli impinging on the whisker array over the course of development may, in turn, impact receptive field structure.

Another possibility is that anisotropic effects on receptive fields are inherent to differences in row vs. arc organization within the neocortex. In rats and mice, it is well-documented that there is a bias towards preferential connectivity among barrels corresponding to whiskers in the same row (Bernardo et al., 1990; Hoeflinger et al., 1995; Kim and Ebner, 1999; Keller and Carlson, 1999), and neurons in barrel cortex typically display patterns of activity that tend to be elongated along the row axis (Armstrong-James and Fox, 1987; Simons, 1978; Kleinfeld and Delaney, 1996; Ego-Stengel et al., 2005; Le Cam et al., 2011). Further, there is evidence for differential effects on responses of S1 neurons along row and arc axes when sensory inputs are altered within the whisker system, for example, through chronic stimulation (Quairiaux et al., 2007) or selective trimming (Dubroff et al., 2005; Wallace and Sakmann, 2008) of specific whiskers. Thus, biases in the functional organization and connectivity within the S1 whisker representation may favor plasticity, preferentially sharpening tuning along the row axis.

A long-standing question has been whether reorganization following sensory loss is primarily driven by deprivation of the lost modality or due to increased experience using the spared senses. Studies in blind humans with Braille reading experience support an important role for tactile experience in generating tactile spatial acuity enhancement following blindness (Wong et al., 2011). The relative contributions of deprivation of the

lost modality versus increased or modified use of the spared senses (Goldreich and Kanics, 2003; Wong et al., 2011; Voss, 2011) to different aspects of cortical reorganization following sensory loss are still not well understood. Our study provides clear evidence for the role of experience in driving compensatory neural and behavioral plasticity following sensory loss, highlighting the importance of therapeutic strategies engaging tactile exploration (for example through play-based learning of tactile skills, Hilditch 2024; or the use of haptic devices, Fleck et al., 2025) to maximize neural and behavioral compensation through touch.

REFERENCES

Abreu MSL, Oliveira LRD (2014) Patterns of arboreal and terrestrial space use by non-volant small mammals in an Araucaria forest of southern Brazil. Anais da Academia Brasileira de Ciências 86:807-819.

Ahl A (1986) The role of vibrissae in behavior: a status review. Veterinary research communications 10:245-268.

Alwis DS, Rajan R (2013) Environmental enrichment causes a global potentiation of neuronal responses across stimulus complexity and lamina of sensory cortex. Frontiers in cellular neuroscience 7:124.

Alwis DS, Rajan R (2014) Environmental enrichment and the sensory brain: the role of enrichment in remediating brain injury. Frontiers in systems neuroscience 8:156.

Antón-Bolaños N, Sempere-Ferràndez A, Guillamón-Vivancos T, Martini FJ, Pérez-Saiz L, Gezelius H, Filipchuk A, Valdeolmillos M, López-Bendito G (2019) Prenatal activity from thalamic neurons governs the emergence of functional cortical maps in mice. Science 364:987-990.

691 Amaral OB, Vargas RS, Hansel G, Izquierdo I, Souza DO (2008) Duration of
692 environmental enrichment influences the magnitude and persistence of its
693 behavioral effects on mice. Physiology & Behavior 93:388-394.
694 Arkley K, Grant RA, Mitchinson B, Prescott TJ (2014) Strategy change in vibrissal active
695 sensing during rat locomotion. Current biology : CB 24:1507-1512.
696 Arkley K, Tiktak GP, Breakell V, Prescott TJ, Grant RA (2017) Whisker touch guides
697 canopy exploration in a nocturnal, arboreal rodent, the Hazel dormouse
698 (Muscardinus avellanarius). Journal of comparative physiology A, Neuroethology,
699 sensory, neural, and behavioral physiology 203:133-142.
700 Bailoo JD, Murphy E, Boada-Saña M, Varholick JA, Hintze S, Baussière C, Hahn KC,
701 Göpfert C, Palme R, Voelkl B, Würbel H (2018) Effects of Cage Enrichment on
702 Behavior, Welfare and Outcome Variability in Female Mice. Front Behav Neurosci
703 12:232.
704 Bartoletti A, Medini P, Berardi N, Maffei L (2004) Environmental enrichment prevents
705 effects of dark-rearing in the rat visual cortex. Nature neuroscience 7:215-216.
706 Beddard FE (1902) Observations upon the Carpal Vibrissæ in Mammals. Proceedings of
707 the Zoological Society of London 72:127-136.
708 Bengoetxea H, Ortuzar N, Bulnes S, Rico-Barrio I, Lafuente JV, Argandona EG (2012)
709 Enriched and deprived sensory experience induces structural changes and rewires
710 connectivity during the postnatal development of the brain. Neural plasticity 2012.
711 Branchi I, D'Andrea I, Santarelli S, Bonsignore LT, Alleva E (2011) The richness of social
712 stimuli shapes developmental trajectories: Are laboratory mouse pups

713 impoverished? Progress in neuro-psychopharmacology & biological psychiatry
714 35:1452-1460.
715 Brecht M, Roth A, Sakmann B (2003) Dynamic receptive fields of reconstructed pyramidal
716 cells in layers 3 and 2 of rat somatosensory barrel cortex. J Physiol 553:243–265.
717 Caires CRS, Bossolani-Martins AL (2023) Which form of environmental enrichment is
718 most effective in rodent models of autism? Behavioural Processes 211:1-8.
719 Cait J, Winder CB, Mason GJ (2024) How much 'enrichment' is enough for laboratory
720 rodents? A systematic review and meta-analysis re-assessing the impact of well-
721 resourced cages on morbidity and mortality. Applied Animal Behaviour Science
722 278:106361.
723 Cancedda L, Putignano E, Sale A, Viegi A, Berardi N, Maffei L (2004) Acceleration of
724 visual system development by environmental enrichment. The Journal of
725 neuroscience : the official journal of the Society for Neuroscience 24:4840-4848.
726 Coq JO, Xerri C (1998) Environmental enrichment alters organizational features of the
727 forepaw representation in the primary somatosensory cortex of adult rats.
728 Experimental brain research 121:191-204.
729 Delciellos AC, Vieira MV (2006) Arboreal walking performance in seven didelphid
730 marsupials as an aspect of their fundamental niche. Austral Ecology 31:449-457.
731 Devonshire IM, Dommett EJ, Grandy TH, Halliday AC, Greenfield SA (2010)
732 Environmental enrichment differentially modifies specific components of sensory-
733 evoked activity in rat barrel cortex as revealed by simultaneous
734 electrophysiological recordings and optical imaging in vivo. Neuroscience
735 170:662-669.

736 Diamond ME, Toso A (2023) Tactile cognition in rodents. Neuroscience & Biobehavioral
737 Reviews 149:105161.
738 Dijkhuizen S, Van Ginneken LMC, Ijpelaar AHC, Koekkoek SKE, De Zeeuw CI, Boele HJ
739 (2024) Impact of enriched environment on motor performance and learning in
740 mice. Scientific Reports 14:5962.
741 Dooley JC, Franca JG, Seelke AM, Cooke DF, Krubitzer LA (2013) A connection to the
742 past: *Monodelphis domestica* provides insight into the organization and
743 connectivity of the brains of early mammals. J Comp Neurol 521:3877-3897.
744 Dooley JC, Krubitzer LA (2019) Alterations in cortical and thalamic connections of
745 somatosensory cortex following early loss of vision. J Comp Neurol 527(10):1675-
746 1688.
747 Ego-Stengel V, e Souza TM, Jacob V, Shulz DE (2005) Spatiotemporal characteristics of
748 neuronal sensory integration in the barrel cortex of the rat. J Neurophysiol
749 93:1450–1467.
750 Engineer ND, Percaccio CR, Pandya PK, Moucha R, Rathbun DL, Kilgard MP (2004)
751 Environmental Enrichment Improves Response Strength, Threshold, Selectivity,
752 and Latency of Auditory Cortex Neurons. Journal of Neurophysiology 92:73-82.
753 Fleck JJ, Zook ZA, Clark JP, Preston DJ, Lipomi DJ, Pacchierotti C, O'Malley MK (2025)
754 Wearable multi-sensory haptic devices. Nature Reviews Bioengineering.
755 Fox K (2003) The origin of cortical surround receptive fields studied in the barrel cortex.
756 Nat Neurosci 6:631–640. Frostig RD (2006) Functional organization and plasticity
757 in the adult rat barrel cortex: moving out-of-the-box. Current opinion in
758 neurobiology 16:445-450.

759 Gallyas F (1979) Silver staining of myelin by means of physical development.
760 Neurological research 1:203-209.
761 Girbovan C, Plamondon H (2013) Environmental enrichment in female rodents:
762 considerations in the effects on behavior and biochemical markers. Behav Brain
763 Res 253:178-190.
764 Goin FJ, Woodburne MO, Zimicz AN, Martin GM, Chornogubsky L (2016) South
765 American Living Metatherians: Physiological Ecology and Constraints. In: A Brief
766 History of South American Metatherians: Evolutionary Contexts and
767 Intercontinental Dispersals, pp 37-75. Dordrecht: Springer Netherlands.
768 Goldreich D, Kanics IM (2003) Tactile acuity is enhanced in blindness. J Neurosci
769 23:3439-3445.
770 Gomez-Pinilla F, Ying Z, Agoncillo T, Frostig R (2011) The influence of naturalistic
771 experience on plasticity markers in somatosensory cortex and hippocampus:
772 effects of whisker use. Brain research 1388:39-47.
773 Graham M, Socha JJ (2020) Going the distance: The biomechanics of gap-crossing
774 behaviors. J Exp Zool A Ecol Integr Physiol 333:60-73.
775 Grant RA, Breakell V, Prescott TJ (2018) Whisker touch sensing guides locomotion in
776 small, quadrupedal mammals. Proceedings Biological sciences 285.
777 Grant RA, Delaunay MG, Haidarliu S (2017) Mystacial whisker layout and musculature in
778 the guinea pig (Cavia porcellus): a social, diurnal mammal. The Anatomical Record
779 300:527-536.
780 Greifzu F, Pielecka-Fortuna J, Kalogeraki E, Krempler K, Favaro PD, Schluter OM, Lowel
781 S (2014) Environmental enrichment extends ocular dominance plasticity into

782 adulthood and protects from stroke-induced impairments of plasticity. Proceedings
783 of the National Academy of Sciences of the United States of America 111:1150-
784 1155.
785 Guic E, Carrasco X, Rodriguez E, Robles I, Merzenich MM (2008) Plasticity in primary
786 somatosensory cortex resulting from environmentally enriched stimulation and
787 sensory discrimination training. Biological research 41:425-437.
788 Hilditch J (2021) Pre-braille Implementation into Early Education: Tactile Activities to
789 Introduce Braille Concepts to Kindergartners. In: Handbook of Disability: Critical
790 Thought and Social Change in a Globalizing World (Rioux MH, Buettgen A, Zubrow
791 E, Viera J, eds), pp 1-31. Singapore: Springer Nature Singapore.
792 Hutson K, Masterton R (1986) The sensory contribution of a single vibrissa's cortical
793 barrel. Journal of neurophysiology 56:1196-1223.
794 Kentner AC, Speno AV, Doucette J, Roderick RC (2021) The Contribution of
795 Environmental Enrichment to Phenotypic Variation in Mice and Rats. eneuro
796 8:ENEURO.0539-0520.2021.
797 Khoo SY-S, Correia V, Uhrig A (2020) Nesting material enrichment reduces severity of
798 overgrooming-related self-injury in individually housed rats. Laboratory Animals
799 54:546-558.
800 Mason G, Clubb R, Latham N, Vickery S (2007) Why and how should we use
801 environmental enrichment to tackle stereotypic behaviour? Applied Animal
802 Behaviour Science 102:163-188.
803 Mieske P, Hobbiesiefken U, Fischer-Tenhagen C, Heinl C, Hohlbaum K, Kahnau P, Meier
804 J, Wilzopolski J, Butzke D, Rudeck J, Lewejohann L, Diederich K (2022) Bored at

home?—A systematic review on the effect of environmental enrichment on the welfare of laboratory rats and mice. Frontiers in Veterinary Science 9.

Molnár Z, Blakemore C (1995) How do thalamic axons find their way to the cortex? Trends Neurosci 18:389–397. 10.1016/0166-2236(95)93935-Q [DOI] [PubMed] [Google Scholar]

Molnár Z, Knott GW, Blakemore C, Saunders NR (1998) Development of thalamocortical projections in the south american gray short-tailed opossum (Monodelphis domestica). J Comp Neurol 398:491–514. 10.1002/(SICI)1096-9861(19980907)398:4%3C491::AID-CNE3%3E3.0.CO;2-Y

Nakhwa AA, Breakell V, Chambers L, Elder A, McLoughlin E, Roberts S, Todd K, Grant RA (2024) Implications of tactile enrichment on the behaviour and whisker movements of four species of carnivorans. Applied Animal Behaviour Science 274:106261.

Jenkins Jr., FA (1974) Tree shrew locomotion and the origins of primate arborealism. In: Jenkins, F.A. (Ed.), Primate Locomotion. Academic Press, New York, pp. 85–115.

Jiang C, Xu X, Yu L, Xu J, Zhang J (2015) Environmental enrichment rescues the degraded auditory temporal resolution of cortical neurons induced by early noise exposure. The European journal of neuroscience 42:2144-2154.

Jones M, Archer M, Dickman C (2003) Predators with Pouches: The Biology of Carnivorous Marsupials: CSIRO PUBLISHING.

Kalogeraki E, Pielecka-Fortuna J, Lowel S (2017) Environmental enrichment accelerates ocular dominance plasticity in mouse visual cortex whereas transfer to standard cages resulted in a rapid loss of increased plasticity. PloS one 12:e0186999.

828 Ladine TA, Kissell RE (1994) Escape Behavior of Virginia Opossums. The American
829 Midland Naturalist 132:234-238.
830 Landers MS, Knott GW, Lipp HP, Poletaeva I, Welker E (2011) Synapse formation in adult
831 barrel cortex following naturalistic environmental enrichment. Neuroscience
832 199:143-152.
833 Lammers AR (2004) The biodynamics of arboreal locomotion in the gray short-tailed
834 opossum (*Monodelphis domestica*).
835 Lammers AR (2007) Locomotor kinetics on sloped arboreal and terrestrial substrates in
836 a small quadrupedal mammal. Zoology (Jena, Germany) 110:93-103.
837 Lammers AR (2009) The effects of substrate texture on the mechanics of quadrupedal
838 arboreal locomotion in the gray short-tailed opossum (*Monodelphis domestica*).
839 Journal of experimental zoology Part A, Ecological genetics and physiology
840 311:813-823.
841 Lammers AR, Biknevicius AR (2004) The biodynamics of arboreal locomotion: the effects
842 of substrate diameter on locomotor kinetics in the gray short-tailed opossum
843 (*Monodelphis domestica*). The Journal of experimental biology 207:4325-4336.
844 Lammers AR, Gauntner T (2008) Mechanics of torque generation during quadrupedal
845 arboreal locomotion. Journal of Biomechanics 41:2388-2395.
846 Lammers AR, Earls KD, Biknevicius AR (2006) Locomotor kinetics and kinematics on
847 inclines and declines in the gray short-tailed opossum *Monodelphis domestica*.
848 The Journal of experimental biology 209:4154-4166.
849 Lazzouni L, Lepore F (2014) Compensatory plasticity: time matters. Frontiers in human
850 neuroscience 8:340.

851 Leah J, Allardyce H, Cummins R (1985) Evoked cortical potential correlates of rearing
852 environment in rats. Biological Psychology 20:21-29.
853 Lee H-K (2023) Metaplasticity framework for cross-modal synaptic plasticity in adults.
854 Frontiers in Synaptic Neuroscience 14.
855 LeMessurier AM, Laboy-Juárez KJ, McClain K, Chen S, Nguyen T, Feldman DE (2019)
856 Enrichment drives emergence of functional columns and improves sensory coding
857 in the whisker map in L2/3 of mouse S1. eLife 8:e46321.
858 Levine JN, Chen H, Gu Y, Cang J (2017) Environmental Enrichment Rescues Binocular
859 Matching of Orientation Preference in the Mouse Visual Cortex. The Journal of
860 neuroscience : the official journal of the Society for Neuroscience 37:5822-5833.
861 López-Bendito G, Aníbal-Martínez M, Martini FJ (2022) Cross-Modal Plasticity in Brains
862 Deprived of Visual Input Before Vision. Annu Rev Neurosci 45:471-489.
863 Lyne A (1958) A thesis on the vibrissae and pelage hairs on the marsupialia and
864 supporting papers.
865 Lyne A (1959) The systematic and adaptive significance of the vibrissae in the
866 Marsupialia. Journal of Zoology 133:79-133.
867 Montgomery, WI (1980) The use of arboreal runways by the woodland rodents,
868 Apodemus sylvaticus (L.), A. flavicollis (Melchior) and Clethrionomys glareolus
869 (Schreber). Mammal Review 10:189-195.
870 Macrini TE (2004) *Monodelphis domestica*. Mammalian Species:1-8.
871 Megevand P, Troncoso E, Quairiaux C, Muller D, Michel CM, Kiss JZ (2009) Long-term
872 plasticity in mouse sensorimotor circuits after rhythmic whisker stimulation. The

Journal of neuroscience : the official journal of the Society for Neuroscience 29:5326-5335.

Mezzera C, López-Bendito G (2016) Cross-modal plasticity in sensory deprived animal models: From the thalamocortical development point of view. Journal of chemical neuroanatomy 75:32-40.

Morland AB, Brown HD & Baseler HA (2021) Cortical reorganization: reallocated responses without rewiring. Current Biology, 31(2), R76-R78.

Muchlinski MN, Durham EL, Smith TD, Burrows AM (2013) Comparative histomorphology of intrinsic vibrissa musculature among primates: implications for the evolution of sensory ecology and "face touch". American journal of physical anthropology 150:301-312.

Mundiñano IC, Martínez-Millán L (2010) Somatosensory cross-modal plasticity in the superior colliculus of visually deafferented rats. Neuroscience 165:1457-1470.

Nakashima AS, Dyck RH (2008) Enhanced plasticity in zincergic, cortical circuits after exposure to enriched environments. The Journal of neuroscience : the official journal of the Society for Neuroscience 28:13995-13999.

Niederschuh SJ, Witte H, Schmidt M (2015) The role of vibrissal sensing in forelimb position control during travelling locomotion in the rat (Rattus norvegicus, Rodentia). Zoology (Jena, Germany) 118:51-62.

Nithianantharajah J, Hannan AJ (2006) Enriched environments, experience-dependent plasticity and disorders of the nervous system. Nature reviews Neuroscience 7:697-709.

895 Piche M, Robert S, Miceli D, Bronchti G (2004) Environmental enrichment enhances
896 auditory takeover of the occipital cortex in anophthalmic mice. The European
897 journal of neuroscience 20:3463-3472.
898 Pocock R (1914) 48. On the Facial Vibrissæ of Mammalia. Journal of Zoology 84:889-
899 912.
900 Polley DB, Chen-Bee CH, Frostig RD (1999) Two directions of plasticity in the sensory-
901 deprived adult cortex. Neuron 24:623-637.
902 Polley DB, Kvasnak E, Frostig RD (2004) Naturalistic experience transforms sensory
903 maps in the adult cortex of caged animals. Nature 429:67-71.
904 Ramamurthy DL, & Krubitzer LA (2016) The evolution of whisker-mediated
905 somatosensation in mammals: Sensory processing in barrelless S1 cortex of a
906 marsupial, *Monodelphis domestica*. Journal of Comparative Neurology 524(17),
907 3587-3613.
908 Ramamurthy DL, Krubitzer LA (2018) Neural Coding of Whisker-Mediated Touch in
909 Primary Somatosensory Cortex Is Altered Following Early Blindness. The Journal
910 of Neuroscience 38:6172-6189.
911 Ramamurthy DL, Dodson HK, Krubitzer LA (2021) Developmental plasticity of texture
912 discrimination following early vision loss in the marsupial *Monodelphis domestica*.
913 Journal of Experimental Biology, 224(9), jeb236646.
914 Ratuski AS, Améndola L, Makowska IJ, Weary DM (2024) Effects of temporary access to
915 environmental enrichment on measures of laboratory mouse welfare. Sci Rep
916 14:15143.

917 Romero-Ferrero F, Bergomi MG, Hinz RC, Heras FJH, de Polavieja GG (2019)
918 idtracker.ai: tracking all individuals in small or large collectives of unmarked
919 animals. Nature Methods 16:179-182.
920 Rupert JE, Schmidt EC, Moreira-Soto A, Herrera BR, Vandeberg JL, Butcher MT (2014)
921 Myosin isoform expression in the prehensile tails of didelphid marsupials:
922 functional differences between arboreal and terrestrial opossums. Anatomical
923 record (Hoboken, NJ : 2007) 297:1364-1376.
924 Sale A, Vetencourt JFM, Medini P, Cenni MC, Baroncelli L, De Pasquale R, Maffei L
925 (2007) Environmental enrichment in adulthood promotes amblyopia recovery
926 through a reduction of intracortical inhibition. Nature neuroscience 10:679.
927 Sale A, Berardi N, Maffei L (2009) Enrich the environment to empower the brain. Trends
928 in neurosciences 32:233-239.
929 Schmitt D, Gruss LT, Lemelin P (2010) Brief communication: forelimb compliance in
930 arboreal and terrestrial opossums. American journal of physical anthropology
931 141:142-146.
932 Seo ML (1992) Effect of environmental complexity on the latency of cortical vibrissa
933 potentials. Developmental psychobiology 25:67-76.
934 Shapiro LJ, Young JW, VandeBerg JL (2014) Body size and the small branch niche: Using
935 marsupial ontogeny to model primate locomotor evolution. Journal of Human
936 Evolution 68:14-31.
937 Sofroniew NJ, Svoboda K (2015) Whisking. Current Biology 25:R137-R140.

938 Taylor JS, Guillery RW (1994) Early development of the optic chiasm in the gray short-
939 tailed opossum, Monodelphis domestica. J Comp Neurol 350:109–121.
940 10.1002/cne.903500108
941 Teichert M, Isstas M, Wenig S, Setz C, Lehmann K, Bolz J (2018) Cross-modal refinement
942 of visual performance after brief somatosensory deprivation in adult mice.
943 European Journal of Neuroscience 47:184-191.
944 Thomas DR, Chadwell BA, Walker GR, Budde JE, VandeBerg JL, Butcher MT (2017)
945 Ontogeny of myosin isoform expression and prehensile function in the tail of the
946 gray short-tailed opossum (*Monodelphis domestica*). Journal of applied physiology
947 (Bethesda, Md : 1985) 123:513-525.
948 van Praag H, Kempermann G, Gage FH (2000) Neural consequences of environmental
949 enrichment. Nature reviews Neuroscience 1:191-198.
950 Voss P (2011) Superior Tactile Abilities in the Blind: Is Blindness Required? The Journal
951 of Neuroscience 31:11745-11747.
952 Voss P (2019) Brain (re)organization following visual loss. WIREs Cognitive Science
953 10:e1468.
954 Wang BS, Feng L, Liu M, Liu X, Cang J (2013) Environmental enrichment rescues
955 binocular matching of orientation preference in mice that have a precocious critical
956 period. Neuron 80:198-209.
957 Wang M, Yu X (2023) Experience-dependent structural plasticity of pyramidal neurons in
958 the developing sensory cortices. Current Opinion in Neurobiology 81:102724.
959 Weissbrod A, Shapiro A, Vasserman G, Edry L, Dayan M, Yitzhaky A, Hertzberg L,
960 Feinerman O, Kimchi T (2013) Automated long-term tracking and social

961 behavioural phenotyping of animal colonies within a semi-natural environment.
962 Nature communications 4:2018.
963 Wilkinson M, Stirton C, McConnachie A (2010) Behavioural observations of singly-housed
964 grey short-tailed opossums (*Monodelphis domestica*) in standard and enriched
965 environments. Laboratory animals 44:364-369.
966 Wong M, Gnanakumaran V, Goldreich D (2011) Tactile spatial acuity enhancement in
967 blindness: evidence for experience-dependent mechanisms. J Neurosci 31:7028-
968 7037.
969 Zheng HJV, Meagher JP, Xu D, Patel YA, O'Connor DH, Kwon HB (2021) Environmental
970 Enrichment Sharpens Sensory Acuity by Enhancing Information Coding in Barrel
971 Cortex and Premotor Cortex. eNeuro 8.
972 Zheng J-J, Li S-J, Zhang X-D, Miao W-Y, Zhang D, Yao H, Yu X (2014) Oxytocin mediates
973 early experience–dependent cross-modal plasticity in the sensory cortices. Nature
974 neuroscience 17:391.
975 Zhu X, Wang F, Hu H, Sun X, Kilgard MP, Merzenich MM, Zhou X (2014) Environmental
976 acoustic enrichment promotes recovery from developmentally degraded auditory
977 cortical processing. The Journal of neuroscience : the official journal of the Society

978 **FIGURE LEGENDS**

979 **Figure 1.** Timeline of experimental manipulations relative to developmental milestones in
980 short-tailed opossums. The four experimental groups are indicated: sSC (standard-reared
981 sighted control), sEB (standard-reared early blind), eSC (enriched sighted), and eEB
982 (enriched early blind). Behavioral and electrophysiological experiments were conducted

983 in adults following the sequence shown in the inset, but ages of adult animals were not
984 strictly matched by postnatal day.

985 **Figure 2. Enriched rearing alters spatial patterns of exploratory behavior. A.**
986 Example movement trajectories from one animal in each experimental group (sEB: light
987 red, eEB: dark red, sSC: light blue, eSC: dark blue) tracked over five minutes during
988 behavioral testing in an enriched arena. **B.** Overlaid movement trajectories from all
989 animals in each experimental group in the arena test show a pattern of increased
990 exploration of vertical vs. horizontal space in opossums reared in enriched cages
991 compared to those reared in standard cages. Plus symbols indicate the center of mass
992 of movement trajectories for each group (colors as in **A**), with data for animals combined
993 within each rearing condition shown in black. **C.** Vertical occupancy profiles during arena
994 exploration. Normalized distributions of vertical position (height above the arena floor)
995 during exploration derived from 1280×720 px video frames (20 px bins used for
996 visualization), pooled across animals (black: enriched, gray: standard; dark gray denotes
997 regions of overlap between the two distributions. **D.** Ethograms showing the temporal
998 structure of locomotor activity and spontaneous crossing events during arena exploration.
999 Horizontal bars indicate periods of activity for representative trials from standard-reared
1000 (top, gray) and enriched-reared (bottom, black) animals. Vertical tick marks denote
1001 spontaneous crossings between surfaces. Time is plotted relative to trial start (mm:ss).
1002 **E-G**. Summary behavioral metrics during arena exploration in standard and enriched
1003 animals. Distributions of vertical preference index (**E**), fraction of trial time spent active
1004 (**F**), and median crossing duration (**G**). Violin plots show Gaussian kernel density
1005 estimates of the pooled distribution for each category; horizontal lines denote medians.

Points represent individual animals, color-coded by experimental group. Animals reared in the enriched environment show significantly a signficant increase in vertical prefernce index. Overall activity levels and duration of crossing events during free exploration were not signficiantly different.

Figure 3. Enriched rearing alters sensorimotor performance during gap crossing. **A.** Experimental setup in the gap crossing task. **B.** Contingency tables showing the percentage of successful and failed gap crossing trials (0% = white, 100% = black; intermediate percentages shown in grayscale) for small (2–10 cm) and large (12–14 cm) gaps under intact and whisker-trimmed conditions, shown separately for each experimental group (sSC, sEB, eSC, eEB). **C.** Number of gap crossings per minute (across all trials) for large and small gaps (with intact or trimmed whiskers). Gap crossing was whisker-dependent in all groups. Data for large gaps after whisker trimming are not shown, as no successful crossings occurred in this condition. **D.** Duration of successful crossings for large and small gaps (with intact or trimmed whiskers). Most groups show significantly longer durations for succesful gap crossing on large gaps (12-14 cm) vs. small gaps (2-10 cm). Upon whisker trimming, most groups show a significant increase in gap crossing duration for small gaps, consistent with the use of whisker-dependent strategies for gap crossing. Enriched blind animals were unique in showing no significant difference between large and small gap durations and no trimming-related increase in small gap crossing times, reflecting enhanced performance on large gaps through whisker use alongside compensatory tactile strategies using other body parts that preserve performance on small gaps when whiskers are absent. For larger gaps, there are prominent differences between experimental groups based on rearing condition and

1029 blindness. Early blind animals crossed gaps faster than sighted controls in standard
1030 conditions, and their performance was further enhanced by enriched rearing. Violin plots
1031 (color-coded by experimental group) show Gaussian kernel density estimates of the data
1032 distribution, with medians indicated by circular markers. See also **Table 2**.

1033 **Figure 4. Enriched rearing amplifies alterations in S1 neuron responses to whisker**
1034 **touch in early blind animals and produces similar shifts in sighted controls. A.**
1035 Spike raster plots from example neurons responsive to whisker touch in each of the four
1036 experimental groups (left to right: sSC, sEB, eSC, eEB). Examples are shown for neurons
1037 with the same best whisker (BW), C2. Trials corresponding to A, B, C, and D whisker
1038 rows are separated by horizontal lines. Within each row, the direction of more rostral ('R')
1039 versus more caudal ('C') whiskers is indicated on the y-axis. **B.** Peristimulus time
1040 histograms (PSTHs) for the same neurons shown in **(A)**. PSTHs corresponding to
1041 whiskers with response magnitudes >50% of the BW response are plotted in black, all
1042 others are in gray. The examples in **(A)** and **(B)** illustrate more selective responses to
1043 whisker touch in standard-reared blind opossums, which is further amplified in enriched
1044 groups. Additionally, neural responses to whiskers vertically adjacent to the BW are
1045 stronger than those for horizontally adjacent whiskers in enriched groups, especially in
1046 enriched early blind opossums. **C.** Spontaneous firing rates of S1 neurons were not
1047 significantly different across experimental groups. **D.** Firing rates evoked by the BW
1048 showed significant differences across experimental groups. Notably, both sighted and
1049 early blind enriched groups showed suppression relative to standard-reared sighted
1050 controls, similar to effects previously reported in early blind animals under standard
1051 rearing conditions. The magnitude of suppression of the BW-evoked response was

1052 greatest in early blind animals reared in the enriched environment. **E.** Mean receptive
1053 field size was significantly smaller in sEB, eSC and eEB animals relative to standard-
1054 reared sighted controls. This is seen both in terms of number of whiskers driving
1055 significant responses (left) and the rank-ordered tuning curve (right) for whisker-
1056 responsive S1 neurons. See also **Table 3**.

1057 **Figure 5. Enriched rearing amplifies anisotropies in receptive fields of S1 neurons**
1058 **in early blind animals, improving selectivity for whisker touch along a behaviorally**
1059 **relevant axis. A.** Schematic of the opossum mystacial whisker pad indicating whisker
1060 rows (light yellow) and arcs (gold), and the horizontal and vertical axes used for receptive
1061 field shape analyses. Insets in individual panels depict the grid of 16 whiskers and the
1062 surrounding whisker (SW) positions included in each analysis, shown for one example
1063 best whisker (BW) position (black filled circle). **B.** Mean two-dimensional somatotopic
1064 receptive fields for each experimental group (left to right: sSC, sEB, eSC, eEB), shown
1065 with 50%, 75%, and 90% contour lines (response levels relative to the BW, smoothed by
1066 linear interpolation for display). This visualization highlights the degree of horizontal vs.
1067 vertical spread (anisotropy) in the average receptive field configuration for each
1068 experimental group. **C-D.** Receptive field shape distributions for S1 neurons in enriched
1069 animals were shifted away from horizontal anisotropic shapes, which are typical of
1070 standard-reared animals. **C** shows receptive field shape distributions when only 1° SW
1071 positions were considered (left) and fractions of horizontally anisotropic receptive fields
1072 corresponding to each group (right). Light gray bars indicate horizontally elongated
1073 receptive fields defined as shape indices > 0, while black bars indicate horizontally
1074 elongated receptive fields with a stricter cutoff of shape indices > 0.5. **D** shows data for

the same neurons when all SW positions (1-3°) were included. Horizontally anisotropic receptive fields are decreased in both enriched groups of animals, and to the greatest extent in enriched early blind animals. **E.** Quantification of tuning width along the row (horizontal/rostrocaudal axis) and arc (vertical axis) across experimental groups. Enriched groups show sharper tuning along the horizontal axis, to a significantly greater extent than standard-reared early blind animals. Enriched groups also show sharper tuning along the vertical axis compared with standard-reared sighted controls, but only to the same extent as previously reported in standard-reared early blind animals. **F.** Distributions of the whisker selectivity index of S1 neurons calculated separately for in-arc whiskers (left) and in-row whiskers (right), when including all SW positions (1°-3°). sEB, eSC and eEB groups all showed significantly greater selectivity for whiskers within arcs, but were not significantly different from each other. The greatest increases in whisker response selectivity were seen for whiskers within rows i.e. the horizontal/rostrocaudal axis, which is the primary axis of natural whisker motion. Selectivity was greatest for eEB animals followed by eSC and sEB animals, with all three of these groups showing significantly higher selectivity along the horizontal axis compared to sSC animals. See also **Table 3**.

MULTIMEDIA

Movie 1. A nesting mother opossum navigating the enriched home cage environment. Movie shown at 4x speed.

Movie 2. Sighted opossum in the arena test. Movie shown at 4x speed.

Movie 3. Early blind opossum in the arena test. Movie shown at 4x speed.

1098 **TABLES**

1099 **Table 1. Experimental Design.** Breakdown of subject information for each experimental
1100 group. Sexes of animals used for electrophysiological recording experiments, total
1101 number of neurons recorded in S1 per group (ALL) and number of S1 neurons with
1102 significant whisker-evoked responses (>2 SD) are listed.

1103 **Table 2. Statistical comparisons for key behavioral results**. Exact p-values for fixed
1104 effects of experimental group and/or test condition obtained from Poisson and Gaussian
1105 generalized linear mixed-effects models, or from Fisher's exact tests for categorical
1106 comparisons, with pairwise contrasts across experimental groups.

1107 **Table 3. Statistical comparisons for key electrophysiological results.** Exact p-
1108 values for fixed effects of experimental group from Gaussian generalized linear mixed-
1109 effects models, with pairwise contrasts across experimental groups.

1110 **EXTENDED DATA FIGURE LEGENDS**

1111 **Figure 1-1. Standard and enriched rearing environments used for short-tailed**
1112 **opossums. A.** Comparison of cages used in standard (left) and enriched (right) rearing
1113 paradigms. Enriched cages (29"l x 18"w x 24"h) were substantially larger (~8x in volume)
1114 than standard cages (8.5"l x 10"w x 8"h), especially in the vertical dimension (~3x). Each
1115 enriched cage contained a nesting box positioned high above the ground, in addition to
1116 the standard nesting cup on the cage floor. Cages also included various enrichment
1117 objects: regularly repositioned manzanita branches, rotating sets of enrichment toys, a
1118 running wheel, and social housing (see *Materials and Methods*). **B.** Frontal view of an
1119 enriched cage. **C.** Top view of the same enriched cage shown in **(B).** Letters mark

individual components visible in both views: nesting box (a), nesting cup (b), food (c), water (d), running wheel (e), manzanita branches (f–l), and enrichment toys (m). **D.** Mother with an attached experimental litter after placement in the enriched rearing environment. **E–F.** Early blind weanling climbing up a branch to reach the nesting box.

Figure 2-1. Behavioral movie analyses. A. Representative frame showing semi-automated identification of an opossum during arena testing using idtracker.ai. **B.** Representative frame showing behavioral tracking in the gap crossing task using DeepLabCut. “IR1” and “IR2” indicate the positions of infrared motion sensors mounted on the edge of each platform, tracked with DeepLabCut to aid in gap crossing analyses. **C.** Zoomed-in view showing an opossum on the start platform extending its whiskers toward the goal platform prior to crossing the gap.

Figure 3-1. Histological verification of recording sites. A, C, E, G. Myelin-stained tangential sections of cortex from a standard-reared sighted (sSC) animal **(A)**, a standard-reared early blind (sEB) animal **(C)**, an enriched sighted (eSC) animal **(E)**, and an enriched early blind (eEB) animal **(G)**. Primary somatosensory cortex (S1) is identifiable as a darkly staining region relative to adjacent cortical fields. **B, D, F, H.** Reconstructions of myeloarchitectural borders drawn from the series of myelin-stained sections in sSC (**B**), sEB (**D**), eSC (**F**) and eEB (**H**) animals. The locations of fluorescent probe insertions are shown as open circles, and recording sites are shown as black filled circles. Only sites at which whisker-evoked neuronal responses were quantified are included. In all panels, medial (M) and rostral (R) directions are indicated by arrows. Scale bar = 250 μm.

EXTENDED DATA TABLES

Table 3-1. ANOVA marginal tests for fixed effects in Figure 3. F statistics, numerator and denominator degrees of freedom (DF1, DF2), and p-values are reported for each model term in analyses corresponding to **Figure 3**.

Table 4-1. ANOVA marginal tests for fixed effects in Figure 4. F statistics, numerator and denominator degrees of freedom (DF1, DF2), and p-values are reported for each model term in analyses corresponding to **Figure 4**.

Table 5-1. ANOVA marginal tests for fixed effects in Figure 5. F statistics, numerator and denominator degrees of freedom (DF1, DF2), and p-values are reported for each model term in analyses corresponding to **Figure 5**.

Figure 1

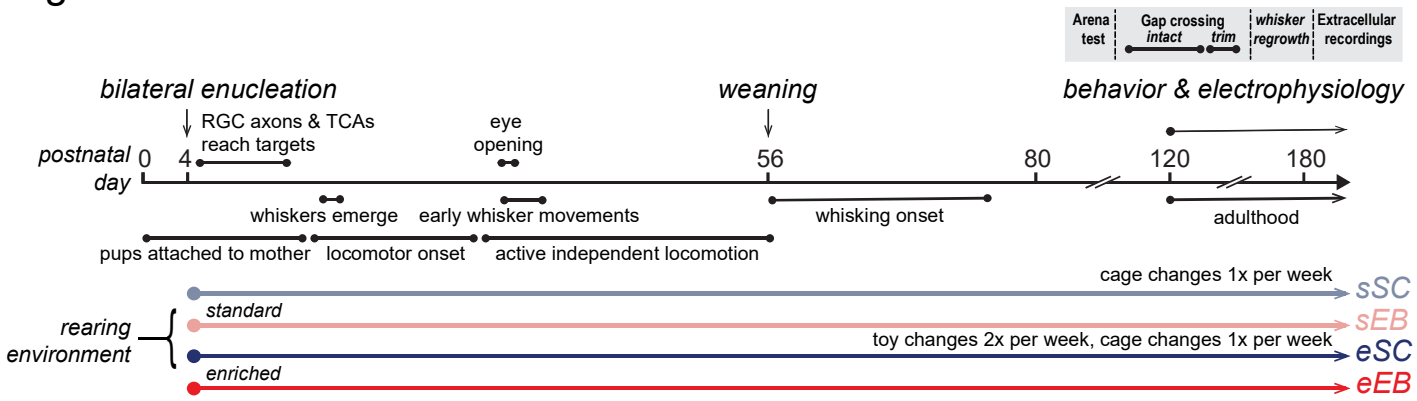
Arena test
Gap crossing
intact
trim
whisker regrowth
Extracellular recordings
bilateral enucleation
weaning
behavior & electrophysiology
RGC axons & TCAs reach targets
eye opening
postnatal day
0
4
56
80
120
180
whiskers emerge
early whisker movements
whisking onset
adulthood
pups attached to mother
locomotor onset
active independent locomotion
cage changes 1x per week
sSC
standard
sEB
rearing environment
toy changes 2x per week, cage changes 1x per week
eSC
enriched
eEB

Figure 2

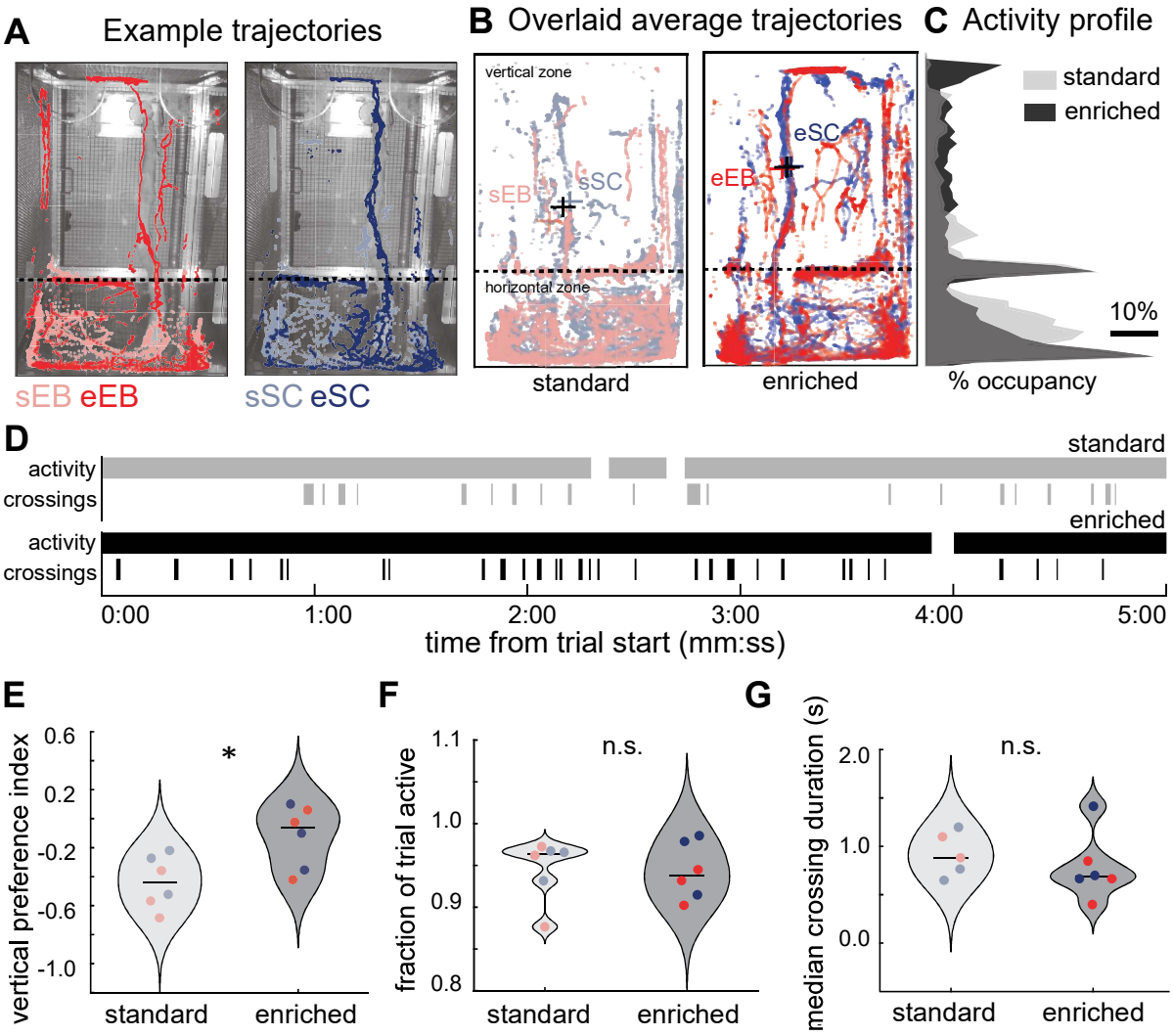
A
Example trajectories
sEB eEB
sSC eSC
B
Overlaid average trajectories
vertical zone
horizontal zone
sEB
sSC
eEB
eSC
standard
enriched
C
Activity profile
standard
enriched
10%
% occupancy
D
activity
crossings
standard
enriched
0:00
1:00
2:00
3:00
4:00
5:00
time from trial start (mm:ss)
E
vertical preference index
0.6
0.2
-0.2
-0.6
-1.0
*
standard
enriched
F
fraction of trial active
1.1
1.0
0.9
0.8
n.s.
standard
enriched
G
median crossing duration (s)
2.0
1.0
0.0
n.s.
standard
enriched

Figure 3

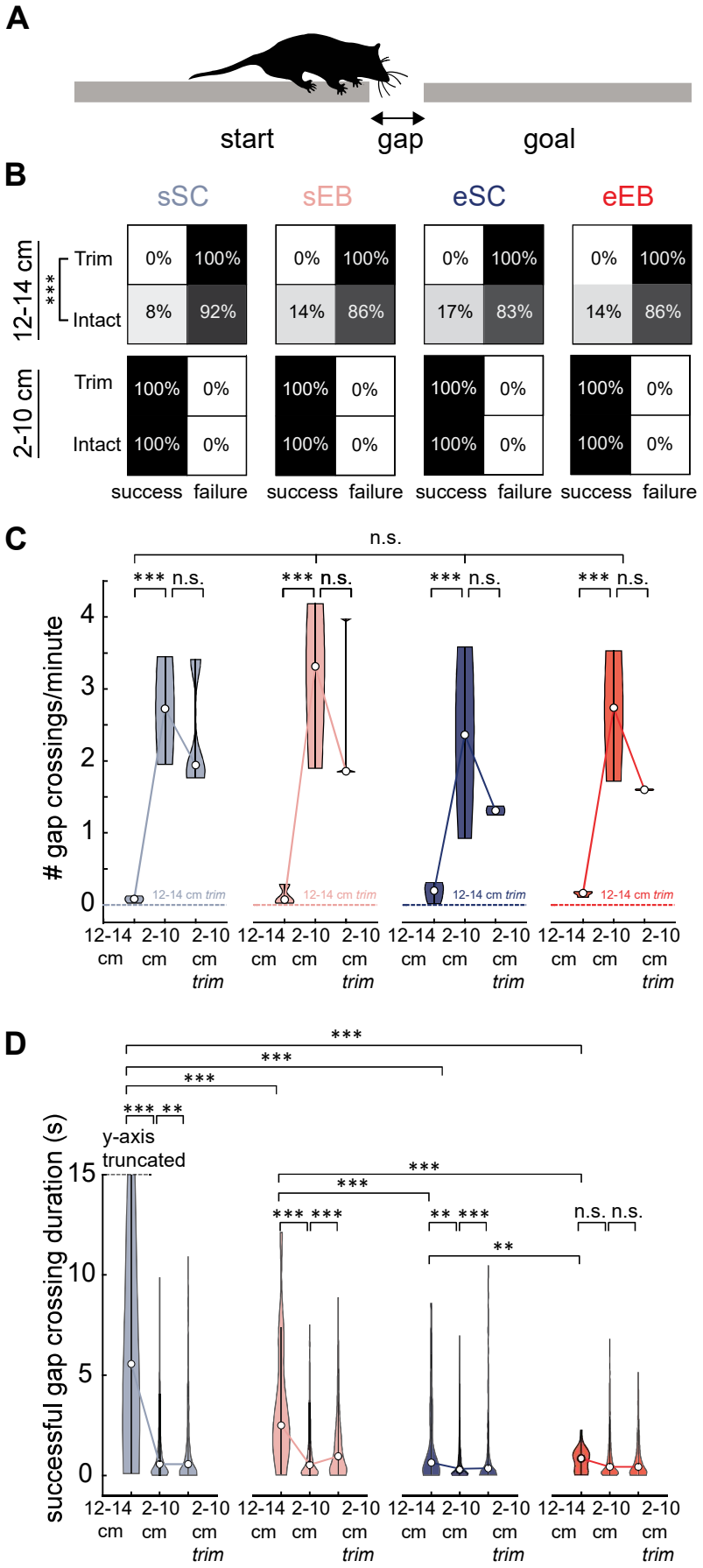
A
start
gap
goal
B
sSC
sEB
eSC
eEB
12-14 cm
Trim
Intact
***
0%
100%
8%
92%
14%
86%
17%
83%
2-10 cm
100%
success
failure
C
n.s.
***
gap crossings/minute
12-14 cm trim
12-14 cm
2-10 cm
2-10 cm trim
D
y-axis truncated
successful gap crossing duration (s)
**

Figure 4

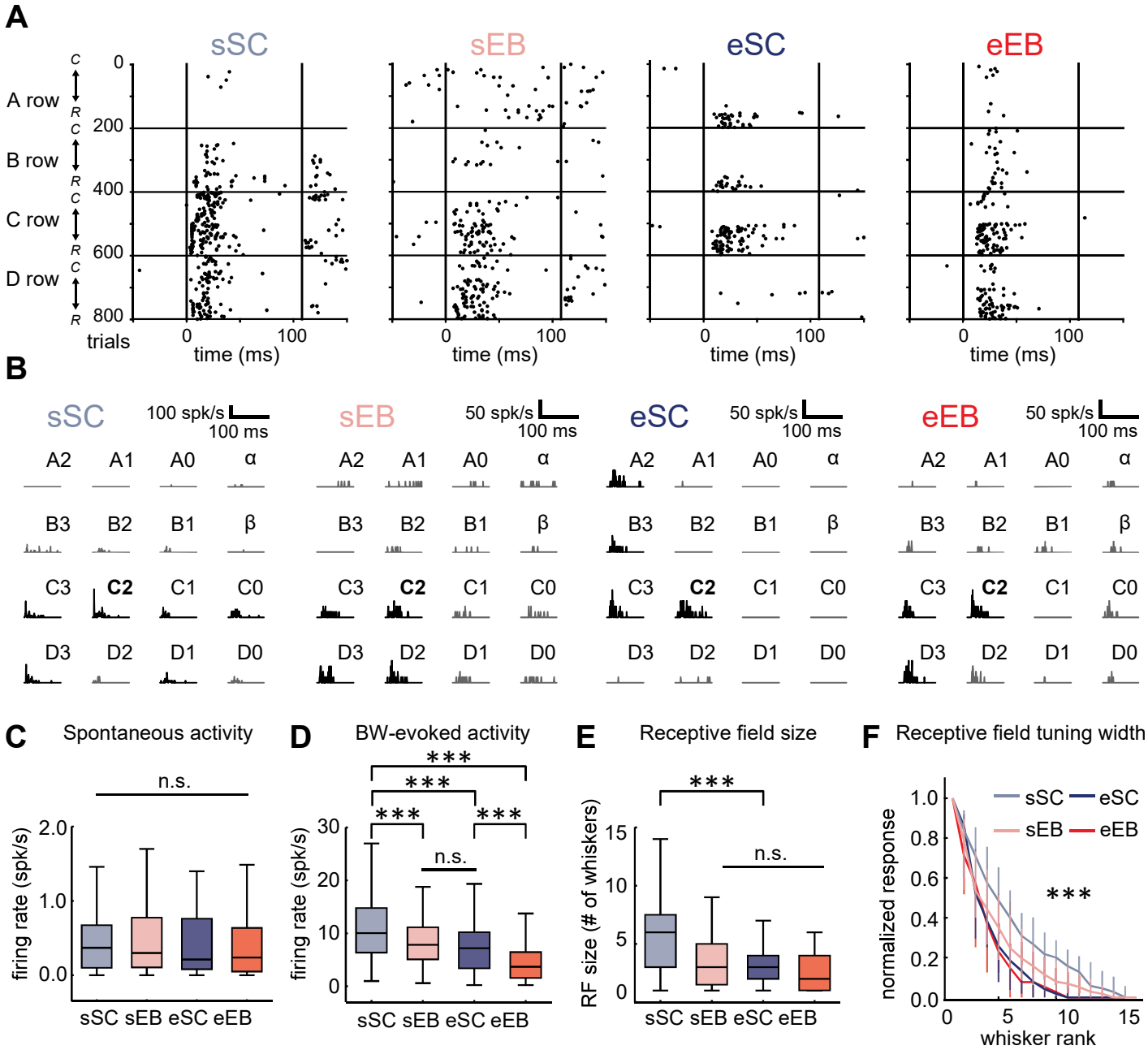
A
sSC
sEB
eSC
eEB
A row
B row
C row
D row
trials
time (ms)
B
100 spk/s
50 spk/s
100 ms
A2 A1 A0 α
B3 B2 B1 β
C3 C2 C1 C0
D3 D2 D1 D0
C
Spontaneous activity
n.s.
firing rate (spk/s)
sSC sEB eSC eEB
D
BW-evoked activity
***
n.s.
E
Receptive field size
RF size (# of whiskers)
F
Receptive field tuning width
normalized response
whisker rank

Figure 5

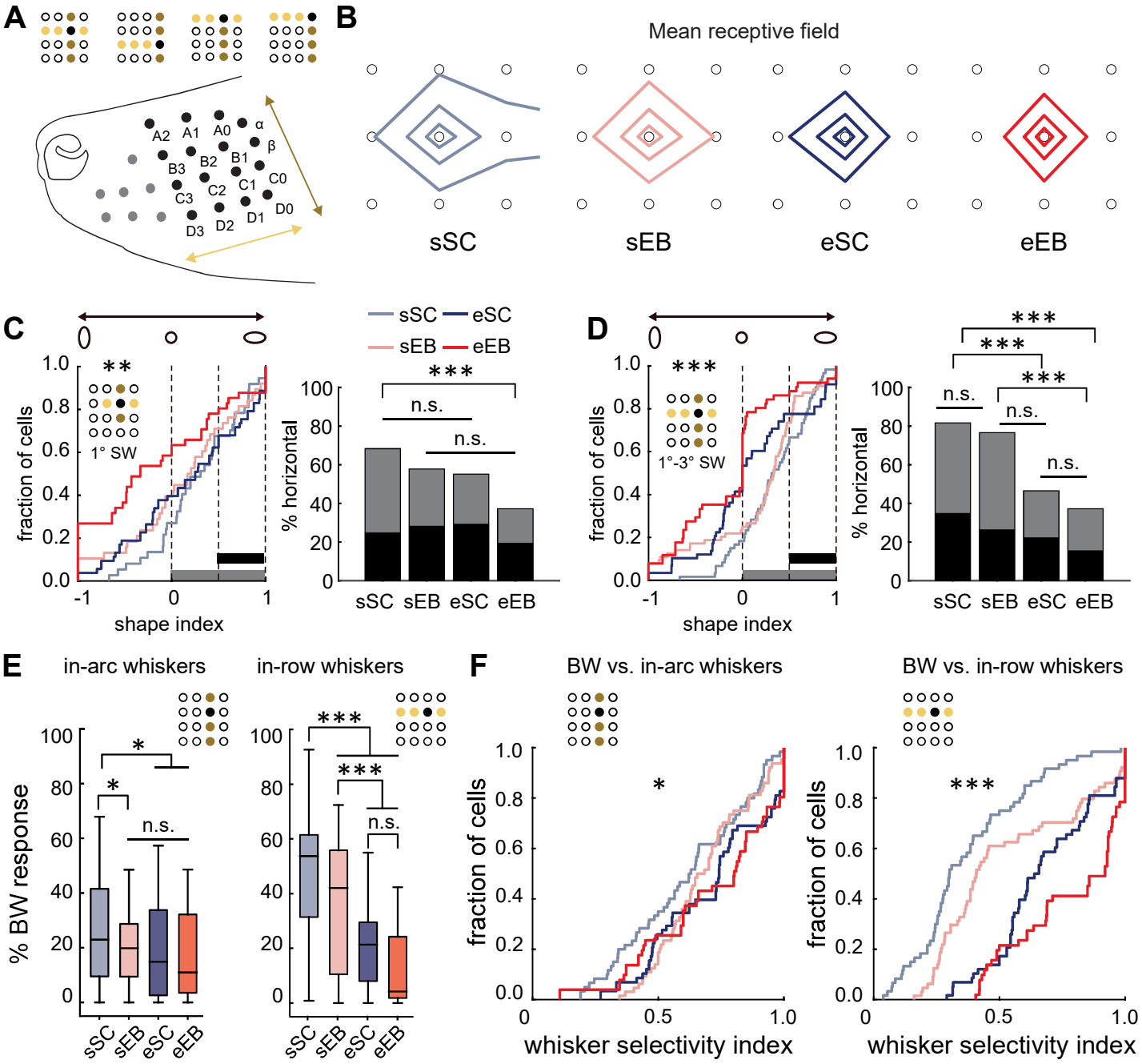
A
A2
A1
A0
α
β
B3
B2
B1
C0
C3
C2
C1
D0
D3
D2
D1
B
Mean receptive field
sSC
sEB
eSC
eEB
C
sSC
eSC
sEB
eEB
1° SW
fraction of cells
shape index
% horizontal
n.s.
D
1°-3° SW
E
in-arc whiskers
in-row whiskers
% BW response
F
BW vs. in-arc whiskers
BW vs. in-row whiskers
whisker selectivity index

Table 1. Experimental Design.

		Visual Condition					
		Sighted (SC)			Early Blind (EB)		
		Sex	ALL	>2 SD	Sex	ALL	>2 SD
Rearing Condition	Standard (s)	5F, 5M	86	60	4F, 5M	88	64
	Enriched (e)	3F, 4M	84	58	3F, 4M	81	51

Breakdown of subject information for each experimental group. Sexes of animals used for electrophysiological recording experiments, total number of neurons recorded in S1 per group (ALL) and number of S1 neurons with significant whisker-evoked responses (>2 SD) are listed.

Table 2. Statistical comparisons for key behavioral results.

Result/ Figure Panel	Fixed Effect p-value	Pairwise comparisons p-values					
	Test Condition	**sSC**		**sEB**		**eSC**	**eEB**
% successful trials **Fig. 2B** Alpha with Bonferroni correction = 0.0125 (1) large vs. small (2) intact vs. trim	-	-		-		-	-
		<2.2e-16		<2.2e-16		<2.2e-16	<2.2e-16
# Gap crossings/minute **Fig. 3C** (1) large vs. small (2) intact vs. trim	2.4277e-09	2.4277e-09		1.7407e-09		9.8418e-10	2.0062e-09
	0.5356	0.5356		0.37091		0.42035	0.15936
Gap crossing duration **Fig. 3D** (1) large vs. small (2) intact vs. trim	1.1011e-79	8.0737e-92		1.4663e-08		0.0128	0.4872
	2.888e-07	0.0081		9.6063e-09		7.2433e-05	0.1481
	Expt. Group	**sSC vs.sEB**	**sSC vs. eSC**	**sSC vs. eEB**	**sEB vs. eEB**	**sEB vs. eSC**	**eSC vs. eEB**
# Gap crossings/minute **Fig. 3C** (3) across groups (large, intact)	0.5927	-	-	-	-	-	-
# Gap crossings/minute **Fig. 3C** (3) across groups (small, intact)		-	-	-	-	-	-
# Gap crossings/minute **Fig. 3C** (3) across groups (small, trim)		-	-	-	-	-	-
Gap crossing duration **Fig. 3D** (3) across groups (large, intact)	6.8796e-51	7.7220e-35	3.6476e-62	3.3333e-72	3.2002e-09	3.8990e-04	0.0021
Gap crossing duration **Fig. 3D** (3) across groups (small, intact)		0.7771	0.0691	2.9099e-14	1.0844e-13	0.1031	7.5517e-05
Gap crossing duration **Fig. 3D** (3) across groups (small, trim)		1.3303e-05	5.6083e-19	6.8960e-15	6.6591e-04	8.6167e-06	0.3183

Exact p-values were obtained from Poisson and Gaussian generalized linear mixed-effects models, or from Fisher's exact tests for categorical comparisons, with pairwise contrasts across experimental groups as indicated (see Methods).

Table 3. Statistical comparisons for key electrophysiological results.

Result/ Figure Panel	Fixed Effect p-value	Pairwise comparisons p-values					
	Expt. Group	sSC vs.sEB	sSC vs. eSC	sSC vs. eEB	sEB vs. eEB	sEB vs. eSC	eSC vs. eEB
Spontaneous activity **Fig. 3C**	0.856	-	-	-	-	-	-
Whisker-evoked activity **Fig. 3D**	4.68e-10	4.53e-04	4.09e-04	1.11e-11	0.939	1.38e-04	3.04e-04
RF size: # of whiskers **Fig. 3E** (left)	1.58-07	9.43e-07	4.29e-06	8.86e-07	0.832	0.763	0.621
Rank-ordered whisker tuning curve **Fig. 3E** (right)	1.55e-25	3.271e-11	1.88e-22	4.04e-19	8.19e-04	0.006	0.618
Shape index: 1st order adjacent whiskers **Fig. 4C** (left)	0.004	0.249	0.445	6.84e-04	0.628	0.023	0.0033
% horizontal: 1st order adjacent whiskers **Fig. 4C** Alpha with Bonferroni correction = 0.008 (right)	-	0.266	0.185	0.001	0.039	0.855	0.083
Shape index: 1st – 3rd order adjacent whiskers **Fig. 4D** (left)	3.45e-05	0.093	0.013	2.19e-06	0.384	0.001	0.016
% horizontal: 1st – 3rd order adjacent whiskers **Fig. 4D** Alpha with Bonferroni correction = 0.008 (right)	-	0.516	9.88e-05	2.00e-06	2.50e-05	7.73e-04	0.340
% BW response: in-arc whiskers **Fig. 4E** (left)	0.042	0.0325	0.0116	0.0244	0.652	0.812	0.848
% BW response: in-row whiskers **Fig. 4E** (left)	8.51e-20	7.10e-05	7.56e-14	1.12e-18	6.19e-05	1.25e-08	0.056
BW vs. in-arc whiskers **Fig. 4F** (left)	0.043	0.080	0.014	0.015	0.436	0.419	0.957
BW vs. in-row whiskers **Fig. 4F** (right)	2.49e-18	2.86e-04	8.18e-12	7.00e-18	3.03e-04	8.31e-09	0.018

Exact p-values were obtained from Gaussian generalized linear mixed-effects models, with pairwise contrasts across experimental groups as indicated (see Methods).